



**THE USE OF MOLECULAR MODELING APPROACHES TO
INVESTIGATE MOLECULAR INTERACTIONS IN
INCLUSION COMPLEXES OF CYCLODEXTRINS**

BY

MS. ORNIN SRIHAKULUNG

**A DISSERTATION SUBMITTED IN PARTIAL FULFILLMENT OF
THE REQUIREMENTS FOR THE DEGREE OF DOCTOR OF
PHILOSOPHY (ENGINEERING AND TECHNOLOGY)
SIRINDHORN INTERNATIONAL INSTITUTE OF TECHNOLOGY
THAMMASAT UNIVERSITY**

ACADEMIC YEAR 2019

COPYRIGHT OF THAMMASAT UNIVERSITY

**THE USE OF MOLECULAR MODELING APPROACHES TO
INVESTIGATE MOLECULAR INTERACTIONS IN
INCLUSION COMPLEXES OF CYCLODEXTRINS**

BY

MS. ORNIN SRIHAKULUNG

**A DISSERTATION SUBMITTED IN PARTIAL FULFILLMENT OF
THE REQUIREMENTS FOR THE DEGREE OF DOCTOR
OF PHILOSOPHY (ENGINEERING AND TECHNOLOGY)
SIRINDHORN INTERNATIONAL INSTITUTE OF TECHNOLOGY
THAMMASAT UNIVERSITY
ACADEMIC YEAR 2019
COPYRIGHT OF THAMMASAT UNIVERSITY**

THAMMASAT UNIVERSITY
SIRINDHORN INTERNATIONAL INSTITUTE OF TECHNOLOGY

DISSERTATION

BY

MS. ORNIN SRIHAKULUNG

ENTITLED

THE USE OF MOLECULAR MODELING APPROACHES TO INVESTIGATE
MOLECULAR INTERACTIONS IN INCLUSION COMPLEXES OF CYCLODEXTRINS

was approved as partial fulfillment of the requirements for
the degree of Doctor of Philosophy (Engineering and Technology)

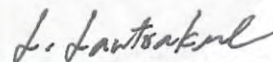
on July 2, 2020

Chairperson



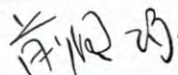
(Associate Professor Waree Kongprawechnon, Ph.D.)

Member and Advisor



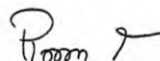
(Associate Professor Luckhana Lawtrakul, Dr.rer.nat.)

Member and Co-advisor



(Professor Ryo Maezono, Ph.D.)

Member



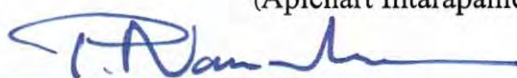
(Associate Professor Pisanu Tooichinda, Ph.D.)

Member



(Apichart Intarapanich, Ph.D.)

Director



(Professor Pruetha Nanakorn, D.Eng.)

Thesis Title	THE USE OF MOLECULAR MODELING APPROACHES TO INVESTIGATE MOLECULAR INTERACTIONS IN INCLUSION COMPLEXES OF CYCLODEXTRINS
Author	MS. ORNIN SRIHAKULUNG
Degree	Doctor of Philosophy (Engineering and Technology)
Faculty/University	Sirindhorn International Institute of Technology/ Thammasat University
Thesis Advisor	Associate Professor Luckhana Lawtrakul, Dr.rer.nat.
Thesis Co-Advisor	Professor Ryo Maezono, Ph.D.
Academic Years	2019

ABSTRACT

Nanoencapsulation of plumbagin (5-hydroxy-2-methyl-1,4-naphthoquinone) using β -cyclodextrin (BCD) and its two derivatives, including dimethyl- β -cyclodextrin (MBCD) and hydroxypropyl- β -cyclodextrin (HPBCD) to form inclusion complex was investigated to prevent the loss of plumbagin in pharmaceutical products, to increase its solubility in water, and reduce the cytotoxicity of the compound. To understand the properties of the complex geometries and the encapsulation process, this research used Molecular docking, Semi-empirical, and Hartree-Fock techniques to simulate the guest/host complexation system of plumbagin/BCD, plumbagin/MBCD, and plumbagin/HPBCD. All calculations were performed using AutoDock4.2.6, GaussView 6.0, and Gaussian 16 software packages. The complex energy, molecular interactions, and insertion pathway of plumbagin/BCDs were examined. The results revealed two different binding modes of the plumbagin molecule inside the BCDs cavity, with 1:1 molecular ratio. In conformation-I, the hydroxyl phenolic group of plumbagin was placed in the BCDs cavity near the narrow-side of the host molecule.

In the other model, conformation-II, the methyl quinone group of plumbagin was placed in the cavity of BCDs near the narrow-side of the host molecule. The intermolecular hydrogen bond, van der Waals, and hydrophobic interactions play an important role in complexation process of plumbagin with BCDs. The structures of plumbagin inclusion complexed with BCD, MBCD and HPBCD in aqueous solution have been investigated by using molecular dynamics simulations, Glycam06 force field run on AMBER18 program. The inclusion structures and the stability of the complexes were also analyzed and validated by thermodynamic properties. The results of molecular dynamics simulations indicate the conformation-II of HPBCD inclusion complex with plumbagin in aqueous solution has better stability than that of the others. Moreover, the releasing directions were also predicted.

Keywords: Cyclodextrin, Hartree-Fock, Inclusion complex, Interaction energy, Molecular docking, Molecular dynamics simulations, Molecular interaction, Nanoscience, Plumbagin, Semi-empirical, Theoretical calculations

ACKNOWLEDGEMENTS

Foremost, I would like to express my sincere gratitude to my advisor Assoc.Prof. Luckhana Lawtrakul for the continuous support of my Ph.D study and research, for her patience, motivation, enthusiasm, and immense knowledge. Her guidance helped me in all the time of research and writing of this thesis. I could not have imagined having a better advisor and mentor for my Ph.D study.

Besides my advisor, I would like to thank the rest of my thesis committee: Assoc.Prof. Waree Kongprawechnon, Assoc.Prof. Pisanu Toochinda and Dr. Apichart Intarapanich, for their encouragement, insightful comments, and hard questions. My heartfelt gratitude is extended to Prof. Ryo Maezono, Japan Advanced Institute of Science and Technology (JAIST), for his critical comments and invaluable suggestions.

My sincere thanks also go to my SIIT friends, Krit Inthajak, Pimonluk Sittikornpaiboon and Kulpavee Jitapunkul for helping and sharing many knowledge and happiness together. Especially, Pornprom Ateetanan and Nitipol Tansakul also cheer me up when I burn out and lack of energy. Including, Mahidol friends, Aniwat Kesorn and Rutchapon Hunkao who are always beside me when I need physic advices. And also, Maezono-lab members for giving me time and encouragement. I appreciate the supporting grants in SIIT-JAIST Dual degree scholarship from the National Electronics and Computer Technology Center (NECTEC), Sirindhorn International Institute of SIIT-JAIST Dual degree scholarship from Technology (SIIT), and Japan Advanced Institute of Science and Technology (JAIST). Last but not least, I would like to give many thanks to my parents, two brothers and Jiradett Kerdsri who have stood by my side.

“Thank you very much”

Ms. Ornin Srihakulung

TABLE OF CONTENTS

	Page
ABSTRACT	(1)
ACKNOWLEDGEMENTS	(3)
LIST OF TABLES	(6)
LIST OF FIGURES	(8)
LIST OF SYMBOLS/ABBREVIATIONS	(12)
 CHAPTER 1 INTRODUCTION	
1.1 Problem Statement	2
1.2 The Objective and Scope	3
1.3 Our Contributions	3
1.4 Computer Software	4
 CHAPTER 2 REVIEW OF LITERATURE	5
2.1 Plumbagin	5
2.2 Cyclodextrin Structure and Physicochemical properties	9
2.3 Inclusion Complexes of cyclodextrins	14
2.4 Molecular Modeling Studies of Inclusion Complexes	18
2.4.1 Semi-empirical	18
2.4.2 Molecular Docking	20
2.4.3 Molecular Dynamics (MD) Simulation	21
 CHAPTER 3 RESEARCH METHODOLOGY	24
3.1 Molecular Structure Construction	24
3.2 Molecular Docking Simulation	25
3.3 Complexation Energy Calculation	26

	(5)
3.4 Molecular Dynamics (MD) Simulation	27
CHAPTER 4 RESULTS AND DISCUSSION	28
4.1 Molecular Docking Calculation	28
4.2 Complexation Energy Calculation	30
4.2.1 Plumbagin/BCD Inclusion Complex	34
4.2.2 Plumbagin/MBCD Inclusion Complex	37
4.2.3 Plumbagin/HPBCD Inclusion Complex	40
4.3 Molecular Dynamics (MD) Simulation	43
4.3.1 Plumbagin/BCD Inclusion Complex	46
4.3.2 Plumbagin/MBCD Inclusion Complex	47
4.2.3 Plumbagin/HPBCD Inclusion Complex	49
CHAPTER 5 CONCLUSIONS	50
REFERENCES	53
APPENDICES	63
APPENDIX A	64
APPENDIX B	66
APPENDIX C	68
APPENDIX D	70
BIOGRAPHY	73

LIST OF TABLES

Tables	Page
2.1 Properties of plumbagin.	7
2.2 Pharmaceutical products containing cyclodextrins, data is taken from literature (Loftsson & Duchene, 2007).	9
2.3 Comparing table of the properties of each type of cyclodextrin (Aree, Hoier, Schulz, Reck, & Saenger, 2000).	13
2.4 β -cyclodextrin and its derivative properties, data is taken from literature (Valle, 2004).	14
2.5 Binding energy range of the similar system which is encapsulated with β -cyclodextrin and calculated with semiempirical calculation.	19
2.6 Literature review of molecular dynamics simulation in the cyclodextrins case studies.	23
4.1 The lowest and the average values of free energy of binding (G) of plumbagin/BCDs inclusion complexes and the number of conformations in a cluster (frequency) obtained from molecular docking calculations at 298.15 K. The starting geometry of the host and guest molecules were calculated by the PM3 method.	29
4.2 The lowest and the average values of free energy of binding (G) of plumbagin/BCDs inclusion complexes and the number of conformations in a cluster (frequency) obtained from molecular docking calculations at 298.15 K. The starting geometry of the host and guest molecules were calculated by the PM6 method.	29
4.3 The lowest and the average values of free energy of binding (G) of plumbagin/BCDs inclusion complexes and the number of conformations in a cluster (frequency) obtained from molecular docking calculations at 298.15 K. The starting geometry of the host and guest molecules were calculated by the PM7 method.	30
4.4 Heat of formation energy (E) and complexation energy (E) in kcal/mol of the minimized inclusion complexes structures from PM6 and PM7	31

4.5 Distance of hydrogen bonds between plumbagin (PL) and three different types of cyclodextrins (BCD, MBCD, and HPBCD) molecules, obtained from PM3, PM6 and PM7 minimized inclusion complex structures	33
4.6 The detail of binding free energies in kcal/mol with the energy components of Plumbagin/CDs inclusion complexes	46



LIST OF FIGURES

Figures	Page
2.1 Benjakul, a Thai traditional plant preparation from PiperchabaLinn., Zingiber of Ficiinale Roscoeorginger., PlumbagaindicaLinn., PiperinterruptumOpiz., and PipersamentosumRoxb, photo are taken from literature (Burodom & Itharat, 2013).	6
2.2 Plumbagin (C ₁₁ H ₈ O ₃ or 5-hydroxy-2-methyl-1, 4-napthoquinone).	7
2.3 The stability test result of plumbagin and piperine in %content, the accelerated condition for testing the Benjakul ethanolic extract was set as 45±2C with 75±3%RH, data is taken from literature (Suthanurak et al., 2010).	8
2.4 α-D-glucopyranose molecule which consists two possible types of chair conformation (I and II) and glycosidic oxygen bridge α (1,4) between two molecules of glucopyranose, figure is taken from literature (Astray, Barreiro, Mejuto, Otero, & Gándara, 2009).	10
2.5 Microstructure of cyclodextrin molecules of glucopyranose. α-cyclodextrin contains 6 molecules of glucoses, β-cyclodextrin with 7 molecules and γ-cyclodextrin with 8 molecules, figure is taken from literature (Sompornpisut, Deechalao, & Vongsvivut, 2002).	12
2.6 Schematic representations of BCD and its deriveritives (MBCD and HP-BCD), which R1 and R2 position were substituted by methyl and hydroxylpropyl- group, adapted from (Alonso, Barreiro, & Díaz, 2015).	14
2.7 Host-guest interaction observed in α-cyclodextrin complex with p- nitrophenol, figure is taken from literature (Dodziuk, 2006).	18
3.1 Schematic representations of glucose unit and atomic numbering of BCD, MBCD HPBCD. All R1 and R2 are substituted by methyl groups on all of the glucose units in MBCD. In HPBCD, only the hydroxyl group at the R1 position of one glucose unit is substituted	25
3.2 Molecular dynamics simulation flowchart (Case, 2018)	27

- 4.1 Schematic representation of two conformations of the inclusion complex. The secondary hydroxyl groups are at the C2 and C3 positions of the BCD, which are located on the wide-side of the truncated cone. The primary hydroxyl group is at the C6 position of the BCD, which is located at the narrow-side of the truncated cone. 28
- 4.2 The complexation energy of six conformations by semi-empirical methods (PCM calculation), including PM3, PM6 and PM7. 32
- 4.3 Energy-minimized structure of the 1:1 plumbagin/BCD complexes in an aqueous environment using polarizable continuum model (PCM). BCD is presented as a line model with a surface, with a probe radius of 1.4 Å. The plumbagin molecule is presented as a stick model. (a) plumbagin/BCD conformation-I obtained from PM3 method, (b) plumbagin/BCD conformation-II obtained from PM3 method, (c) plumbagin/BCD conformation-I obtained from PM6 method and (d) plumbagin/BCD conformation-II obtained from PM6 method, (e) plumbagin/BCD conformation-I obtained from PM7 method and (f) plumbagin/BCD conformation-II obtained from PM7 method. 35
- 4.4 Hydrogen bonds in 1:1 plumbagin/BCD complexes. (a) plumbagin/BCD conformation-I obtained from PM3 method, (b) plumbagin/BCD conformation-II obtained from PM3 method, (c) plumbagin/BCD conformation-I obtained from PM6 method, (d) plumbagin/BCD conformation-II obtained from PM6 method, (e) plumbagin/BCD conformation-I obtained from PM7 method and (f) plumbagin/BCD conformation-II obtained from PM7 method. 36
- 4.5 Energy-minimized structure of the 1:1 plumbagin/MBCD complexes in an aqueous environment using polarizable continuum model (PCM). MBCD is presented as a line model with a surface, with a probe radius of 1.4 Å. The plumbagin molecule is presented as a stick model. (a) plumbagin/MBCD conformation-I obtained from PM3 method, (b) plumbagin/MBCD

conformation-II obtained from PM3 method, (c) plumbagin/MBCD conformation-I obtained from PM6 method and (d) plumbagin /MBCD conformation-II obtained from PM6 method, (e) plumbagin/MBCD conformation-I obtained from PM7 method and (f) plumbagin/MBCD conformation-II obtained from PM7 method.

38

4.6 Hydrogen bonds in 1:1 plumbagin/MBCD complexes. (a)

plumbagin/MBCD conformation-I obtained from PM3 method, (b) plumbagin/MBCD conformation-II obtained from PM3 method, (c) plumbagin/MBCD conformation-I obtained from PM6 method, (d) plumbagin/MBCD conformation-II obtained from PM6 method, (e) plumbagin/MBCD conformation-I obtained from PM7 method and (f) plumbagin/MBCD conformation-II obtained from PM7 method.

39

4.7 Energy-minimized structure of the 1:1 plumbagin/HPBCD

complexes in an aqueous environment using polarizable continuum model (PCM). HPBCD is presented as a line model with a surface, with a probe radius of 1.4 Å. The plumbagin molecule is presented as a stick model. (a) plumbagin/HPBCD conformation-I obtained from PM3 method, (b) plumbagin/BCD conformation-II obtained from PM3 method, (c) plumbagin/HPBCD conformation-I obtained from PM6 method and (d) plumbagin/HPBCD conformation-II obtained from PM6 method, (e) plumbagin/ HPBCD conformation-I obtained from PM7 method and (f) plumbagin/HPBCD conformation -II obtained from PM7 method.

41

4.8 Hydrogen bonds in 1:1 plumbagin/HPBCD complexes. (a)

plumbagin /MBCD conformation-I obtained from PM3 method, (b) plumbagin/HPBCD conformation-II obtained from PM3 method, (c) plumbagin/HPBCD conformation-I obtained from PM6 method, (d) plumbagin/HPBCD conformation-II obtained from PM6 method, (e) plumbagin/HPBCD conformation-I obtained from PM7 method and (f) plumbagin/HPBCD conformation

-II obtained from PM7 method.	42
4.9 RMSD plots of all six inclusion complexes, where the inclusion complexes, CDs and plumbagin are highlight by black, blue, and red, respectively.	45
4.10 Distance between the center of mass of plumbagin with BCD and two derivatives.	46
4.11 Two conformations illustration of BCD inclusion complexes: (left) bound form (right) intermediate along the releasing pathway.	47
4.12 Two conformations illustration of MBCD inclusion complexes: (left) bound form (right) intermediate along the releasing pathway.	48
4.13 Two conformations illustration of HPBCD inclusion complexes: (left) bound form (right) intermediate along the releasing pathway.	49



LIST OF SYMBOLS/ABBREVIATIONS

Symbols/Abbreviations	Terms
ACD	α -Cyclodextrin
ACFDT	Adiabatic-Connection Fluctuation-Dissipation Theorem
BCD	β -Cyclodextrin
B3LYP	Becke, 3-Parameter, Lee-Yang-Parr
CDs	Cyclodextrins
GCD	γ -Cyclodextrin
HF	Hartree-Fock
HF-SCF	Hartree-Fock Self-Consistent Field
HPBCD	Hydroxyl Propyl- β -Cyclodextrin
HOMO	Highest Occupied Molecular Orbital
LUMO	Lowest Unoccupied Molecular Orbital
MBCD	Methyl- β -Cyclodextrin
MD	Molecular Dynamics
NCI	The National Cancer Institute
NDDO	Neglect of Diatomic Differential Overlap
NDO	Neglect of Differential Overlap
PB	Plumbagin
PCM	Polarizable Continuum Model
PM3	Parameterization Method 3
PM6	Parameterization Method 6
PM7	Parameterization Method 7
SCF	Self-Consistent Field
vdW	van der Waals

CHAPTER 1

INTRODUCTION

Thai herbs are economically important plants, which can be distributed in high quality and usable products for the market, from pharmaceuticals, cosmetics, and food production. These products are related to challenging issues such as the compound instability, lack of aromatic permanence (e.g. perfumes), and other issues related to chemical and physical properties of the products. An important issue is that of the preservation of these products, which can lead complications in the production line and increase the cost of the product. Additionally, the use of herb products is required in a very large quantity, since there is no transformation or extraction of the active compound to be used directly. Usage of Thai herbs involves a greater number of herbs and frequency to get equally desired effects as Chinese herbs and other traditional medicines. As a result, the packaging of Thai herb products is usually larger in quantity and volume, which can inflate the transportation costs and the shelf space in the logistic system. In addition, there are difficulties and complications in its usage, which requires a novel technology to address these problems more efficiently. Some expensive rare herbs or active compounds such as Sandalwood, Agarwood, and off-season plants usually suffer from product shortage. In addition, they are unable to maintain a good condition due to the deterioration from air and sunlight, which can diminish the price and quality of these substances.

Consequently, the use of the highly effective and affordable technique of nanoencapsulation is recommended to prolong the period of compound retention and to provide protection from sunlight and humidity. Moreover, this technique can efficiently decrease the amount of herb used in the initial product, thus reducing the cost and increasing the value of herbal products. In the nanoencapsulation scheme, a 'guest' molecule is encapsulated or inserted inside a 'host' molecule, which protects it from harmful external factors. The inter-molecular interaction between 'guest' and 'host' is the key, since it determines much about the resulting 'host-guest inclusion complex'. A primary predictor in this mechanism is the binding energy, the existing potential energy between these molecules. It can be directly translated into how easily

these complexes form when ‘guest’ and ‘host’ molecules interact with one another, as well as how difficult it will be to coax the ‘host’ molecule to release the ‘guest’ when, for example, drugs need to be delivered to the target system.

Molecular modeling techniques are currently widely used in chemistry and pharmacology to obtain insight into information at the molecular level of systems of interest. The computational results help explaining the molecular interactions and predict the mechanisms that govern the processes when experimental techniques are insufficient. The computational models can predict and screen the results when varying the compounds or the system conditions prior to laboratory tests. Semi-empirical quantum mechanical calculations have been successful for descriptions in organic chemistry because some parameters are approximated or generalized to simplify the calculations or to yield a result based on experimental data. Modern semi-empirical quantum mechanical models such as Parameterization Method 3, 6 and 7 (PM3, PM6 and PM7) are often used to explore the electronic structure dependent properties of large molecules, where *ab initio* electronic structure methods (without approximations) are too expensive (Stewart, Császár, & Pulay, 1982).

The main purpose of this study was to investigate the binding formation and the release path of plumbagin of β -cyclodextrin (BCD) and its derivatives. Consequently, the structural and dynamics properties were determined by using Molecular Dynamics (MD) simulations in aqueous solution. The MM-GBSA were used to predict binding energy of the inclusion complexes. Furthermore, the releasing mechanisms were investigated to gain more information to select the most suitable host for plumbagin with enhanced bioavailability.

1.1 Problem Statement

The main problem of this work is the instability of the active compounds or plumbagin in Benjakul. The compounds in Thai medicinal plants easily sublime and lose their properties. Plumbagin is unstable and very reactive with sunlight and sensitive to temperature. Therefore, we have to keep it under low temperature (-20°C), because of the low melting point of plumbagin at $76-78^{\circ}\text{C}$. As a result, those conditions increase

the complexity and cost of the production process to preserve the anti-cancer activity of these compounds.

1.2 The Objective and Scope

In this work, the molecular interactions of a plumbagin inclusion complex with β -cyclodextrin (BCD), dimethyl- β -cyclodextrin (MBCD), and hydroxypropyl- β -cyclodextrin (HPBCD) were investigated. To understand the properties of the complex geometries and the encapsulation process, this research used semi-empirical methods and molecular dynamics simulation methods to describe the complexation of plumbagin/BCD, plumbagin/MBCD, and plumbagin/HPBCD systems in water. The complex energy, molecular interactions, and insertion pathway of plumbagin/BCDs were examined.

1.3 Our Contributions

Many possibilities exist for the geometry of the host-guest complex, and the optimization of such structures are too expensive for *ab initio* methods. Ideally, a few candidate conformations need to be selected from all the possible host-guest geometry configurations, while keeping a reasonable computational cost. This selection process is the most challenging part in this work. Our approach is to employ a semi-empirical evaluation of the possible geometries by running docking calculations. The Lamarckian genetic algorithm is utilized in order to find the ideal candidate conformations. The host molecule is considered fixed in a vacuum, while the guest molecule is allowed to have a free range of movement. One hundred movements of the guest molecule are performed. The final geometries are collated and classified into groups of possible conformations, each with calculated values of binding energy and frequency of occurrence. The value is the basis of selecting appropriate candidate conformations considered for calculation. From the results, we extract two possible conformations, based on the geometry orientation of the methyl group in plumbagin with respect to the wider rim of the fixed host molecules. With the three types of host molecules considered in this study, a total of 6 structures are selected for the calculations. After performed MD simulations, we have found that the plumbagin molecule is encapsulated near the

center of all host molecules. HPBCD with conformation-II expresses the lowest binding energy.

1.4 Computer Software

All of the semi-empirical (PM3, PM6 and PM7) calculations described in this dissertation were carried out by using Gaussian 16 (Frisch et al., 2016) program. GaussView 6.0 (Milla, 2009) program package was used for final structural visualization and constructing a small molecule, electronic structure and energies of atoms, molecules, and surfaces which can produce various results by using semi-empirical and PCM calculations. For Molecular Docking calculations, AutoDock 4.2.6 (Morris et al., 2009) was performed the calculation. For MD simulations, AMBER18 (Case et al., 2018) program was employed. UCSF Chimera (Pettersen et al., 2004) program is used for visualization in the movement of our system in the solution.

CHAPTER 2

REVIEW OF LITERATURE

The focus of previous researches (Srihakulung et al., 2017), is in the domain of active compound or plumbagin (Guest). The study aims to find a suitable host to preserve this active compound in nanocapsule or cyclodextrin (Host). The research studied the β -cyclodextrin (BCD) and its derivatives which are widely used in many industries, especially pharmaceuticals. In this chapter, the study elaborates the literature review of the previous related works about the target systems, as well as the interaction between them. The study will focus on the properties of the electrostatic force affecting two compounds to bind together and to form the inclusion complex.

2.1 Plumbagin

Plumbagin (5-hydroxy-2-methyl-1, 4-naphthoquinone) is an organic compound extracted from the *Plumbago indica* root (Araújo, Melo, Júnior, & Albuquerque, 2016). Plumbagin has anti-microbial, neuroprotective, and anti-carcinogenic properties and is generally used in Thai herbal medicines (Paiva, Figueiredo, Aragão, & Kaplan, 2003). There are some reports using BCD and HPBCD to form a 1:1 inclusion complex with plumbagin to increase its solubility in water and reduce the cytotoxicity of the compound (Oommen, Shenoy, Udupa, Kamath, & Devi, 1999; Souza, Singh, Aithal, & Udupa, 1997; Singh & Udupa, 1997). Unfortunately, no experimental papers report the use of MBCD as a host for encapsulation with plumbagin.

The guest molecule is plumbagin, which is one of the biological active compounds of Benjakul. Benjakul is a Thai traditional formula being used in many applications including: health balancing and adaptogen drug for cancer patients. It consists of five traditional herbs, including fruit of *Piperchaba*, root of *Pipersamentosum*, stem of *Piperinterruptum*, rhizome of *Zingiber of ficinale*, and root of *Plumbago* in the same weight ratio as shown in Figure 2.1. Healer use these traditional recipes as an adaptogenic to balance body element in patients (Rattarom, Sakpakdeejaroen, & Itharat, 2010).



Figure 2.1 Benjakul, a Thai traditional plant preparation from *Piperchaba*Linn., *Zingiber of Ficiinale Roscoe*orginger., *Plumbagaindica*Linn., *Piperinterruptum*Opiz., and *Pipersamentosum*Roxb, photo are taken from literature (Burodom & Itharat, 2013).

Benjakul also applied for cancer patients in order to provide the body balance and improve the immunity before the chemotherapy (Saetung, Itharat, Dechsukum, Wattanapiromsakul, & Keawpradub, 2005). It also contains anti-inflammatory effect by inhibiting the cytokine releasing in an inflammatory process induced by LPS *in vitro* study (Burodom & Itharat, 2013). Five plant ingredients were collected and dried at 50°C in oven. Next, the ethanolic extraction process began with mixing 100 g of each dried-plants component. After that, we ground the plants into rough powder, then macerated with 95% ethanol. This solution was filtrated and concentrated under the reduced-pressure condition. The extract compound was kept at -20°C until start the experiments (Burodom & Itharat, 2013). From the criteria by the National Cancer Institute guidelines (NCI) , the cytotoxic activity of extracts and pure substance with IC₅₀ values < 30 µg/ml and < 4 µg/ml. Plumbagin is an active compounds, which can provide the best cytotoxic activity against lung cancer (Rattarom et al., 2010). The structure of the active compound molecule is shown in Figure 2.2.

The notation of plumbagin rooted from the plant *Plumbago* (Vijver, 1972), while its molecule is from *Nepenthes* and *Genera–Drosera*, carnivorous plant (Rischer, Hamm and Bringmann, 2002). Plumbagin is an organic compound with the chemical formula of C₁₁H₈O₃ or (5-hydroxy-2-methyl-1, 4-naphthoquinone) with the potentials of neuroprotective (Son et al., 2010), and inhabit ectopic growth (Sugie et al., 1998), such as anti-breast cancer (Sugie et al., 1998) and anti-lung cancer (Hsu, 2006).

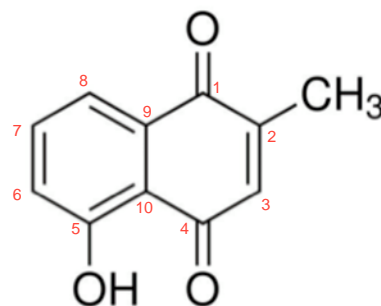


Figure 2. 2 Plumbagin ($C_{11}H_8O_3$ or 5-hydroxy-2-methyl-1, 4-naphthoquinone).

Plumbagin structure consists naphthoquinone, which contains two oxygen atoms at 1-4 position. One methyl group substitution at 2 positions and one Hydroxyl group substitutes at position 5. Generally, there is one problem with both active compounds, especially in plumbagin which is the instability related to their low melting point (76-78°C) (Suthanurak, Sakpakdeejaroen, Rattarom and Itharat, 2010). The study illustrated the degradation of two active compounds as shown in Figure 2.3. From this figure, plumbagin degrades from 100% to 28.70% within 2 months. On the other hand, piperine sublimates only 5% during the same period of time.

Table 2.1 Properties of plumbagin.

Properties	Plumbagin
Molecular formula	$C_{11}H_8O_3$
Molecular weight	188.18
Density (g/cm^3)	1.354
Melting point ($^{\circ}C$)	76-78
Boiling point ($^{\circ}C$)	383.9
Solvent solubility	Soluble in alcohol, acetone, benzene, acetic acid and slightly soluble in hot water 79 $\mu g/mL$
Stability	Stable in closed place under dry and well ventilated, but incompatible with strong oxidizing agents
Lipophilicity	$\log P$ 3.04

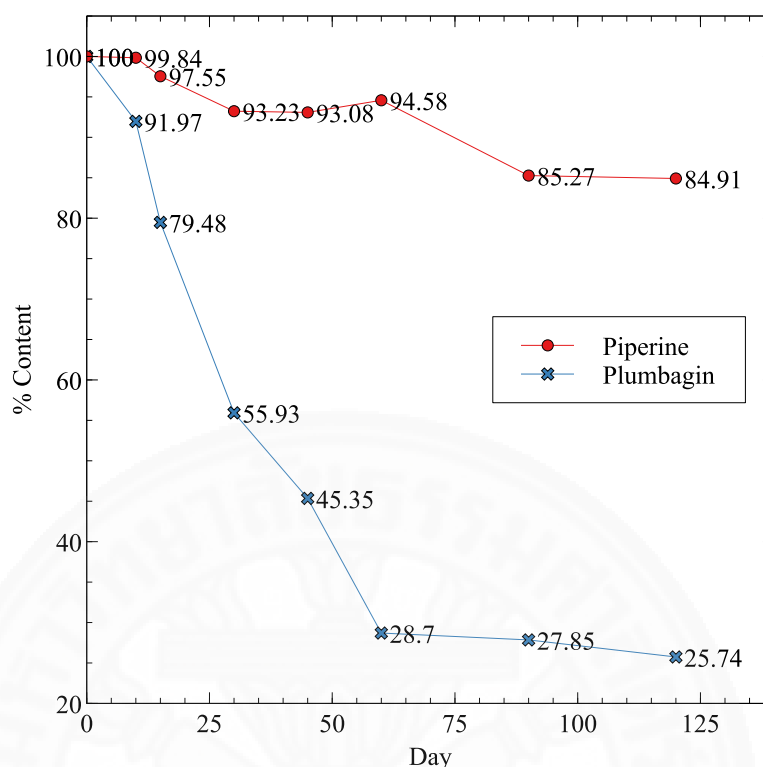


Figure 2.3 The stability test result of plumbagin and piperine in %content, the accelerated condition for testing the Benjakul ethanolic extract was set as $45 \pm 2^\circ\text{C}$ with $75 \pm 3\%\text{RH}$, data is taken from literature (Suthanurak et al., 2010).

The degradation of plumbagin is the main problem that we are focusing in this study. The issue from instability of active compounds can be resolved by encapsulation technique similar to other compounds in the pharmaceutical industry. This technique has normally been used for protecting the ingredients and controlling active compound's releasing rate. The protection has also used to prevent the degradation from the light and oxygen or retard evaporation (Risch, 1995). Commonly, there are several types of the encapsulations. Cyclodextrin is one of the technique that can be used for the encapsulation of the drug that contains hydrophobic properties and the drug delivery through aqueous diffusion-controlled barriers (Rasheed, Kumar and Sravanthi, 2008). Therefore, cyclodextrin is one of the techniques to effectively prevent the degradation or sublimation of the compounds.

2.2 Cyclodextrin Structure and Physicochemical properties

Cyclodextrins, discovered over a century (Villiers, 1891), are the production of the starch interacted with an enzyme and can be used as the pharmaceutical excipients and complexing agents which can improve the aqueous solubility, stability and bio-availability of the active compound. Cyclodextrins is a natural cyclic oligosaccharide, that recently accessible as pharmaceutical excipients. Many commercialized drugs nowadays are presented in Table 2.2 (Loftsson & Duchene, 2007).

Table 2.2 Pharmaceutical products containing cyclodextrins, data is taken from literature (Loftsson & Duchene, 2007).

Drug/Cyclodextrin	Trade Name	Formulation	Company/Country
PGE 2/BCD	Prostarmon E	Sublingual tablet	Ono, Japan
PGE 1/ACD	Prostavastin	infusions	Schwarz, Germany, USA
OP-1206/ACD	Opalmon	Tablet	Ono, Japan Chiesi, Italy
Piroxicam/BCD	Brexin, Flogene Cicladon	Suppository Liquid	several European countries Ache, Brasil
Benexate HCl/BCD	Ulgut Lonmie	Capsule	Teikoku, Japan Shionogi, Japan
Chlordiazepoxide/BCD	Transillium	Tablet	Gador, Argentina
Hydrocortisone/HPBCD	Dexocort	Solution	Actavis, Iceland
Itraconazole/HPBCD	Sporanox	Solution	Janssen, Belgium and USA
Cisapride /HPBCD	Propulsid	Suppository	Janssen, Belgium
17 β -Estradiol/RMBCD	Aerodioli	Nasal Spray	Servier, France
Chloramphenicol/MBCD	Clorocil	Eye drop solution	Oftalder, Portugal
Dextromethorphan/BCD	Rynathisol		Synthelabo, Italy

Cyclodextrins are made from natural products that constructed by digestable cellulose. The cyclic oligosaccharide consists of (α -1, 4)-linked α -D-glucopyranose. The center of the cavity in cyclodextrins has lipophilic properties and hydrophilic at outer surface of the structure. Chair conformation of glucopyranose holds together with oxygen, and their orientation structure like cone as shown in Figure 2.4. The α -, β - and γ -cyclodextrin compose 6, 7 and 8 glucopyranose units (Dass & Jessup, 2000). Glucopyranoses are in chair conformation, which can affect the cyclodextrins' shape likes a truncated cone rather than the cylinders. The primary hydroxyl groups position is at the narrow edge (C6), on the other hand the secondary hydroxyl groups (C2) and (C3) are at the wider rim of the cone. The apolar C3 and C5 hydrogens and ether-like are inside of the cone which can cause the central cavity to contain a lipophilic property. The outside molecule shows hydrophilic character, which can dissolve in water. As the result, the cavity of cyclodextrins can form the inclusion complexes with a wide and various of guests that contain a hydrophobic character. From this property, several researches and works have used this useful functionality in many applications.

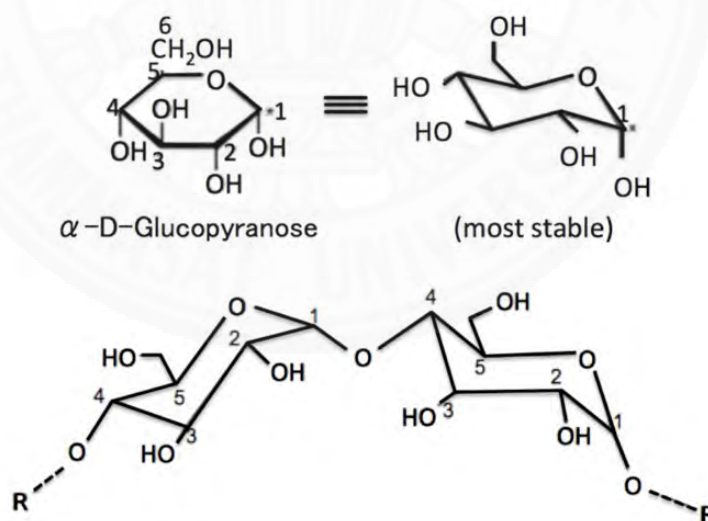


Figure 2.4 α -D-glucopyranose molecule which consists two possible types of chair conformation (I and II) and glycosidic oxygen bridge $\alpha(1,4)$ between two molecules of glucopyranose, figure is taken from literature (Astray, Barreiro, Mejuto, Otero, & Gándara, 2009).

There are several applications of cyclodextrins that can make the CDs suitable for applications in the field of analytical chemistry, pharmaceutical and food (Singh, Sharma, & Banerjee, 2002), such as:

- Sensitive substances (oxygen or light) stabilization;
- Substances (pigments or color) masking;
- Degradation of substances protection using micro-organisms;
- Liquid substances to powders modification;
- Chemical reactivity (guest molecules) modification;
- Volatile substances fixation;
- Ill smell and taste masking;
- Cyclodextrins with guest molecules catalytic activity.

Basically, there are 3 types of cyclodextrin, which can be categorized into 3 main types: α -cyclodextrin, β -cyclodextrins and γ -cyclodextrin, derived from the first generation (parent cyclodextrins). The most accessible and economical type, β -cyclodextrin, is commonly the most applicable in several industries. On the other hand, α -cyclodextrin contains the least steric strain, while γ -cyclodextrin contains the highest strain (Szejtli, 1998). Modifications can improve some of the properties as shown in the Table 2.3, consisting of the stability against oxygen or light, solubility, and also aids in controlling the guest molecules chemical activity. Otherwise, the cavity volume is always the first property to consider to make it proper with the host, however, it is an optional than optimal solubility and safety data (Rajewski & Stella, 1996).

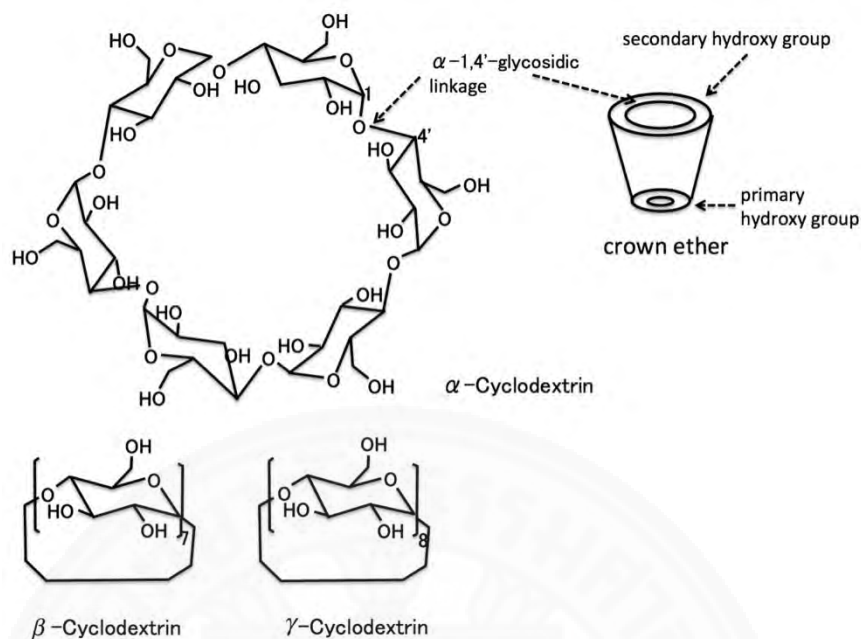


Figure 2.5 Microstructure of cyclodextrin molecules of glucopyranose. α -cyclodextrin contains 6 molecules of glucoses, β -cyclodextrin with 7 molecules and γ -cyclodextrin with 8 molecules, figure is taken from literature (Sompornpisut, Deechalao, & Vongsvivut, 2002).

Because of the 6 Å of cavity in BCD, it is suitable for accommodating for aromatic groups. Therefore, many drug molecules were encapsulated by BCD molecule. From the previous work, the molecular modeling through molecular docking studies (Dandawate et al., 2014) and the experimental studies (Singh & Udupa, 1997) have shown that plumbagin molecule is normally selected to form the inclusion complex with β -cyclodextrin (BCD). Similar to the recent research from Sinlikhitkul, Toochinda, Lawtrakul, Kuropakornpong, and Itharat (2019), this study showed that only BCD and GCD can form the inclusion complex with plumbagin (the evidence from XRD, FTIR, DSC and TGA). This solubility study indicates that BCD can form the complex in a wide range of concentration without agglomeration. Hence, this research is focusing on the inclusion complex, which are formed between plumbagin and BCDs molecules.

β -cyclodextrin is a nontoxic cyclic oligosaccharide comprising seven α -D-glucoses (Qi & Hedges, 1997). The inner hydrophobic cavity of BCD consists of carbon and hydrogen atoms. The rims of the cavity comprise primary and secondary hydroxyl

groups, giving it a hydrophilic property. The secondary hydroxyl groups are at the C2 and C3 positions of the cyclodextrin (CD), which is located on the wide-side of the truncated cone. The primary hydroxyl group is at the C6 position, which is located at the narrow-side of the truncated cone (Connors, 1997). Methylated β -cyclodextrin and hydroxypropyl- β -cyclodextrin are BCD derivatives that are widely used in drug encapsulation because of their inclusion ability and high water solubility (>500 mg/mL) while the solubility in water of BCD is 18.5 mg/mL at 25°C (Loftsson & Duchene, 2007).

Table 2.3 Comparing table of the properties of each type of cyclodextrin (Aree, Hoier, Schulz, Reck, & Saenger, 2000).

Properties	ACD	BCD	GCD
Molecular weight	972	1,135	1,297
Glucose monomers	6	7	8
Internal cavity diameter (Å)	4.7-5.3	6.0-6.6	7.5-8.3
Water solubility (g/L @T=25°C)	14.2	18.5	23.2
Melting range (°C)	255-260	255-265	240-245
Water of crystallization	10.2	13-15	8-18
Water molecules in cavity	6	11	17
Cavity volume (mL/mol)	174	262	472
Price (US/g pharma grade)	1.0	0.025	0.8

From the parent cyclodextrins, many cyclodextrins derivatives have been further synthesized. The productions of the derivatives are aminations, esterifications of primary and secondary hydroxyl groups of the cyclodextrins. The differences of groups and number of substitutions can make the properties of derivatives to change from their parents. Normally, all derivatives can change hydrophobic cavity volume. The improvement of solubility, stability and chemical interaction of guest molecules are gained. In this research, the BCD contains the suitable cavity size with plumbagin, however the limitation of solubility is the main problem of BCD (18.5 g/L). As a result, the derivatives are considered in this research with correlated two factors:

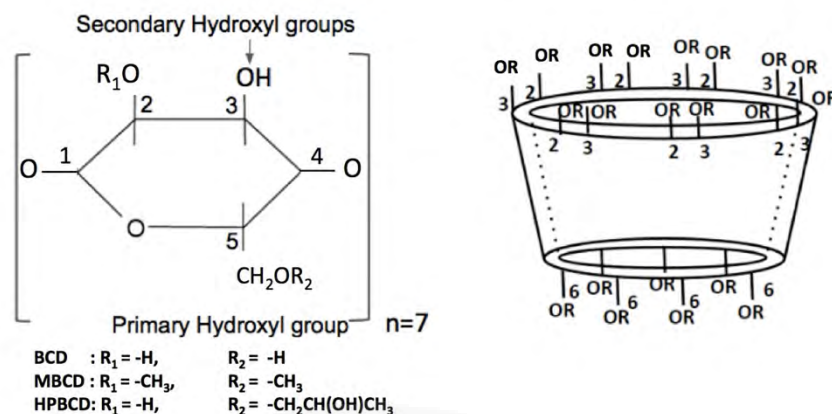


Figure 2.6 Schematic representations of BCD and its derivatives (MBCD and HPBCD), which R1 and R2 position were substituted by methyl and hydroxylpropyl-group, adapted from (Alonso, Barreiro, & Díaz, 2015).

Table 2.4 β -cyclodextrin and its derivative properties, data is taken from literature (Valle, 2004).

Information	BCD	MBCD	HPBCD
Product name	Beta-cyclodextrin	Methyl-beta-cyclodextrin	Hydroxylpropyl-beta-cyclodextrin
Chemical formula	$C_{42}H_{70}O_{35}$	$C_{56}H_{98}O_{35}$	$C_{45}H_{76}O_{36}$
CAS#	7585-39-9	128446-36-6	94035-02-6
Molecular weight	1135	1310	1454
Melting point ($^{\circ}C$)	260	180-182	305
Flash point ($^{\circ}C$)	-	187	-
Bulk Density	-	400 kg/m ³	-
Water solubility (g/L @T=25 $^{\circ}C$)	18.5	> 500	> 600
Price (USD/g)	0.025	111.880	7.078

2.3 Inclusion Complexes of cyclodextrins

The prominent point of cyclodextrins is the forming property of the inclusion complex between host and guest in a wide range, even in the solid, liquid and gas phases (Villiers, 1891). The guest molecules are held in the cavity of cyclodextrins. The lipophilic cavity of cyclodextrins offer the proper environment to non-polar of the host to form the inclusion complex (Magnusdottir, Másson, & Loftsson, 2002). The host and guest binding is in a dynamic equilibrium, and the strength of binding is related to how suitable between host and guest are, also specific local interactions of their surface

atoms. The ability of formation of the inclusion complex between cyclodextrins and guest is a function of two key factors:

1. Steric or spatial arrangement of atoms in molecules that related to size of cyclodextrins cavity and guest. For instance, if the guest's size is larger than the host's cavity, they are unable to fit properly.
2. The thermodynamic interaction between host and guest, for favorable case, the driving force of the total energy is shown in negative value that will pull the guest into the cyclodextrins.

Primarily, energetically supportive interactions consist of four types that can shift the equilibrium in order to form the inclusion complex:

1. Repulsive interactions decrement from the water environment and hydrophobic guest;
2. Hydrogen bonds increasing formed as displaced water depart to the larger pool;
3. Polar water molecules displacement from a non-polar cavity;
4. Hydrophobic interactions rising by inserting guest into polar CD cavity.

To form complex, the initial equilibrium is quite accelerated (in a minute), while on the other hand, the final equilibrium is time consuming to reach. Several techniques can be used to form the inclusion complexes, depending on the active compound (guest), equilibrium kinetics, processes and other ingredients. The interactions between host-guest molecules contains four types, which are all non-covalent interaction. This interaction involves more dispersed variations of electromagnetic interactions between molecules or within a molecule, not sharing electron. Four types of interaction are consisted of:

1. hydrogen bond

The hydrogen bond between host-guest molecule can be categorized into two types including:

- O-H, N-H and F-H, hydrogen bond donors between cyclodextrin' hydroxyl groups with a guest molecule, which mostly restricted to the primary O(6)-H side. Because of the more flexible of the primary side than the secondary O(2) and O(3).

- C-H \cdots O hydrogen bond: C-H bond is a weaker hydrogen bond donor than O-H, N-H and F-H bonds. However, their donor potential could not be ignored (ca 2-8 kJ/mol) (Saenger & Steiner, 1998). C-H bond are of importance in many organic systems, because the O-H, N-H and F-H bonds are more polarized than C(sp³)-H in pure hydrocarbons. The charge of H atom of the methyl group (C(sp³)-H) is +0.13, where the charge of H atom of the hydroxyl group (O-H) is +0.34 (Sterten Kjell; Mæland, Inge, 1982). Normally, C-H \cdots O interaction appears between polar guest with the cavity lining of host molecules. According to the MP2/6-311++G(d, p) computations (Qingzhong, Wang, & Zhiwu, 2007), the estimated interaction energies are slightly above 4 kJ/mol, which is a quarter to a third of conventional hydrogen bonds.

2. Electrostatic interactions

The electrostatic includes all of the electrostatic forces such as, force between the permanent charge or between dipoles as well as multipoles. Electrostatic interactions consist of three important types: ion-ion, ion-dipole and dipole-dipole interaction. For the cyclodextrin inclusion complex system, therefore cyclodextrin normally exists as neutral molecules. In addition, the cyclodextrin is substituted with some appropriately functional group.

The ion-dipole interactions of the cyclodextrin system normally increase from the ionic charge of the guest molecule. Some guests consist of the dianions such as SO₄²⁻ or CO₃²⁻, which can be an increase binding force from the tight bond with cyclodextrins. The dipole moments of cyclodextrin were studied, and the range between 10-20 D is suggested as a highly polarized (Sakurai, Kitagawa, Hoshi, Inoue, 1990). Normally, the cyclodextrin complex contains a small dipole moment in the range of 2-4 D, which obtain from PM3 computations (Liu, Li, Song, & Guo, 2000). The large dipole moment plays an important role in the inter molecular interaction in this system. For dipole-dipole interactions, many studies about several substitution benzene derivative of guest

which expresses dipole (Hehre, 2003; Messiad, Yousfi, Djemil, & Guebailia, 2016). Their dipoles are anti parallel to host molecule. The dipole-dipole interaction plays an important role to stabilize the complex, and it related to the orientation of the guest molecule.

3. Van der Waals interactions

Van der Waals (vdW) interaction or London dispersion interaction consists of the combination between induction and dispersion interaction and only dispersion interaction. Nowadays, this interaction is the important evident which are responsible for many phenomena in physics, chemistry and biology. While vdW interaction is much weaker force comparing with ionic, metallic and covalent bonding, but this force plays an important role to determine the stabilities and structures of various compounds. Many researches express about vdW force play an important role of the cyclodextrin inclusion complex system. Normally the hydrophobic interactions between two non-polar molecules provide a positive enthalpy process, on the other hand, van der Waals interactions are observed as in the opposite. The negative enthalpy occurs in the van der Waals case. According to van der Waals interaction in cyclodextrin inclusion complexes, many works consider this system in gas phase to avoid the solvent effect. While they concluded that vdW interaction is the major contribution to form then inclusion complexes.

4. Hydrophobic interaction

Hydrophobic interaction in CDs complexation is an underdiscussing problem. Normally, hydrophobicity was specified to be the results of enhanced structure of the water molecules in the near vicinity of the non-polar solution, and it would cause large entropy loss during the hydration. In experiments, non-polar molecules associated in water normally with the positive enthalpy and positive entropy changes. This seems like a signature of hydrophobic interaction. The fact that most of the experimental enthalpy and entropy

alterations of CD complexation are negative seems to show that the hydrophobicity is not an important force in CD inclusion complex.

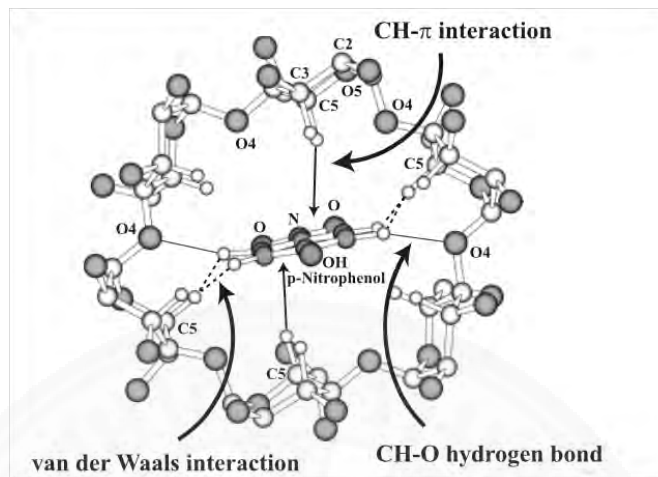


Figure 2.7 Host-guest interactions observed in an α -cyclodextrin complex with *p*-nitrophenol, figure is taken from literature (Dodziuk, 2006).

2.4 Molecular Modeling Studies of Inclusion Complexes

If we consider the interaction between host and guest molecule directly, it does not relate to only size and shape molecule. Since our system consists of neutral guest and host, dipole-dipole interaction plays the important role in intermolecular interaction. The non-covalent interactions are stabilized in the inclusion complex molecules. Therefore, the different models provide the various results. In this research, three computational tools were used to investigate in the research.

2.4.1 Semi-empirical quantum mechanical method

Generally, quantum mechanical methods can be classified as *ab initio* or semi-empirical methods. In *ab initio* method, the calculations are derived directly from theoretical principle, no experimental data included. On the other hand, semi-empirical methods are the simplified versions of Hartree-Fock theory by using empirical or experimental data for the correction in order to improve the performance of the calculation by considering the electron-electron interactions when the molecules overlap density between two orbitals or as known as Neglect of Differential Diatomic Overlap (NDDO), and also the experimental data such as heat of formation, molecular

geometries, dipole moments, and ionization potentials were used for parametrizations. As a result, these calculations by using the semi-empirical method is faster than *ab initio* calculation. Semiempirical calculations are also very successful for the organic systems, that contain a few elements (C, H, N, O, Si, S, P) in used and the very large molecular size.

From a literature review, some researches have been studied the inclusion complexes of cyclodextrins with various guest with semi-empirical methods as shown in Table 2.5 . The total stabilization energies of a molecule usually between 1 and 20 kcal/mol, which are considered as small binding energy compared to a covalent bond energy = 100 kcal/mol. To describe non-covalent interactions, the accurate methods of quantum chemistry are required. Semi-empirical provide binding energy with the huge range. The binding energies of PM3 are in the range of -33.19 to -3.36 kcal/mol. For PM6 is between -21.68 to 5.38 kcal/mol. PM7 is between -53.17 to -51.89 kcal/mol.

Table 2.5 Binding energy range of the similar system which is encapsulated with β -cyclodextrin and calculated with semiempirical calculation.

Method	Guest	Binding energy (kcal/mol)	Reference
PM3	Linalool	-12.58 to -7.02	(Lawtrakul, Inthajak, & Toochinda, 2014)
	Eugenal	-9.72 to -7.57	(Lawtrakul, Inthajak, & Toochinda, 2014)
	Methyl eugenol	-13.53 to -10.09	(Lawtrakul, Inthajak, & Toochinda, 2014)
	Estragole	-7.01 to -5.39	(Lawtrakul, Inthajak, & Toochinda, 2014)
	Eugenol	-12.77	(Lawtrakul, Inthajak, & Toochinda, 2014)
	PNBA1	-9.80 to -8.20	(Leila, Sakina, Bouhadiba, Fatiha, & Leila, 2011)
	PNBA2	-33.19 to -21.88	(Leila et al., 2011)
PM6	Sulfonamide	-4.45 to -3.36	(Seridi, Seridi, Berredjem, & Kadri, 2013)
	Carvacrol	-25.12 to -23.09	(Abdelmalek et al., 2016)
	Tyrosine	-21.68 to -18.19	(Bouhadiba et al., 2017)
	Sulfonamide	2.94 to 5.38	(Seridi et al., 2013)
	Ortho-Anisidine	-13.50 to -13.20	(Djilani et al., 2014)
PM7	Tyrosine	-53.17 to -51.89	(Bouhadiba et al., 2017)

2.4.2 Molecular Docking

There are many possible conformations, that host and guest can be formed. The different initial geometry will provide the difference results. If there are some tools, that can predict the possible conformation must be easier to select the complex to run further calculations. AutoDock is one of the most popular program packages for molecular docking simulations, by which one can predict how match between ligand and the host which is the biomacromolecular molecule from the interaction between them. Normally this program is used in computer-aided drug design to find candidate molecules with their targets.

AutoDock 4.2.6 predicts the best way for the interaction between two molecules using two components including scoring function and search methods. First, scoring functions commonly parameterized against a data set of empirically determined binding affinities between the molecules. AutoDock comprises several search method algorithms, however for AutoDock 4.2.6, the Lamarckian Genetic Algorithm (LGA) was found to be the optimal solution. LGA explores the conformational states of a flexible guest and utilizes the maps produced by AutoGrid to evaluate the interaction of the host and guest at every point of the docking simulation. The energy evaluation measures the consistency of individuals. The search method stops when the energy reaches the maximum.

From my literature review, many researches which related to the CD inclusion complexes system also performed docking simulations to predict the possible conformation of their works. Dandawate et al., 2014 studied also used docking simulations to predict the interactions and orientations of plumbagin and PLIHZ with BCDs. The binding energy of plumbagin and BCD is computed to be -4.9 kcal/mol with two hydrogen bonds between these two molecules by using AutoDock Vina software. Similar to Zhang et al., his study compared the result of docking simulations with the experiment result of BCD and HPBCD with phloridzin. The lowest binding energy of HPBCD from docking calculation coincided with the experimental values (UV, FT-IR and ^1H NMR spectra).

2.4.3 Molecular Dynamics (MD) Simulation

For our system, the medicine will be taken into the body, and it will transport into the target cell. That means the environment is full of water molecules under the body temperature. For further analysis, the additional implementation of the system to make it resemble the actual environment is very important, which can help us understand the behavior of our system. Molecular Dynamic simulations are appropriate tools to investigate dynamic systems and setting the system into more realistic conditions (thermodynamic condition). Therefore, we need to design the suitable constraints, and the calculation should account for the available computational power. Simulation size (n = number of particles), timestep, and total time duration must be selected so that the simulations can finish within a reasonable time period. However, the simulations should be long enough to be relevant to the time scales of the natural processes being studied.

Shaikh et al., 2017 investigated Albendazole with BCD, HPBCD and SBEB CD, the MD part are calculated by AMBER14 programs with AMBER force field. TIP3P water model was used to solvate the complex molecules in a truncated octahedron box with the edge of solvent box 12.0 Å. Total step for three cycles is 50,000 steps, 20,000 steps were steepest descents and 30,000 steps were conjugate gradient with non-bonded interaction. The system heated from 0 to 300 K with collision frequency of 2.0 ps for 1ns. After heating the system were equilibrated under NVT ensemble. The coordinated were saved every 5,000 steps (10 ps). All bonds involving hydrogen atoms were restrained using SHAKE algorithm.

Carvalho et al., 2018 studied 17- α -methyltestosterone encapsulated with BCD with 1:2 ratio by using AMBER12 program. The complex molecules were built by Glycam06h and using AMBER force field (GAFF version 1.4). The inclusion complexes were optimized by using *ab initio* HF/6-31G* calculations. All molecules were solvated by a cubic box of TIP3P water molecules. The closeness parameter is 10 Å away from the boundary of a CD and the guest molecule. The energy minimization is considered the system was heated from 298 to 300 K during 300 ps. Further the system was equilibrated for another 200 ps both under constant volume conditions

(NVT). After that it followed a 200 ps equilibration at 298 K and 1.0 atm (NPT). Longer production runs were carried out for 50 ns at 298 K and 1.0 atm (NPT ensemble).

Zhang et al., 2018 studied solubility of antimicrobial activity of alamethicin in aqueous solution by complexation with γ -Cyclodextrin. They performed the calculation by using NAMD 2.10 program. Their molecules were solvated in a cubic box of water using the solvate package implemented in VMD. The box size is 2.0 nm. TIP3P model was used for surrounding water. The system was minimized in 1,000 steps and heated from 0 to 303 K. The cutoff of switching function was set to 12.0 Å. The CHARMM36 force field was used.

Sangpheak et al., 2015 work want to improve the solubility and the biological activities of PNS by forming inclusion complexes with BCD and its derivatives, heptakis-(2,6-di-O-methyl)- β -cyclodextrin (2,6-DM β CD) and (2-hydroxypropyl)- β -cyclodextrin (HP β CD). The GROMACS package (version 4.6.5) program was used for MD simulations by using Glycam06 carbohydrate FF and its modified force field. The inclusion complex surrounded with approximately 3,200 SPC water molecules in a cubic box of $4.5 \times 4.5 \times 4.5$ nm³ the whole system was minimized with 50,000 steps with the steepest descent algorithm (SD) and then 20,000 steps with the conjugated gradient algorithm (CG). Under periodic boundary condition with an NPT ensemble, the system was heated at a constant temperature of 298 K for 1 ns.

Hanpaibool et al., 2018 study the encapsulation of Genistein with BCD in the water solution. They run MD calculation by using AMBER program by Glycam06 force field for carbohydrates. The complexes were solvated by SPC water molecules within a distance of 12 Å from the system surface resulting in ca. 1,420 water molecules in a ca. $41 \times 41 \times 41$ Å³ truncated octahedron periodic box. The system was heated up to 298 K with the relaxation time for 100 ps. All systems were simulated using NPT ensemble at constant pressure of 1 atm and temperature of 298 K for 100 ns.

Table 2.6 Literature review of molecular dynamics simulation in the cyclodextrins case studies.

Cyclodextrin	Guest	Solvent	Water model	Force field	Program	Ensemble	T (K)	Time	Reference
BCD	Eugenol	water	-	-	In house (Fortran)	T	298	360.63 ps	(Alvira, 2018)
BCD	Patchouli Alcohol	water	TIP3P	-	AMBER11	-	273	2 ns	(Xu et al., 2017)
BCD, HPBCD	Albendazole	water	TIP3P	AMBER	AMBER14	NVT	300	1 ns	(Shaikh et al., 2017)
BCD	17- α -methyl-testosterone (MT)	water	TIP3P	AMBERGAFF version 1.4	AMBER12	NVT, NPT	298	50 ns	(Carvalho et al., 2018)
GCD	Alamethicin	water	TIP3P	CHARMM36	NAMD 2.10	NPT	303	270/200/800 ns	(Zhang et al., 2018)
BCD	Eucalyptol	water 2,000 molecules	simple-point charge (SPC)	GLYCAM06h	AMBER14	NPT	298	100 ps	(Nutho, Nunthaboot, Wolschann, Kungwan, & Rungrotmongkol, 2017)
BCD	Genistein	water 1,420 molecules	SPC	GLYCAM06	AMBER	NPT	298	100 ns	(Hanpaibool et al., 2018)
BCD, 2,6-DMBCD and HPBCD	Pinostrobin	water 3,200 molecules	SPC	GLYCAM06	GROMACS 4.6.5	NPT	298	1 ns	(Sangpheak et al., 2015)

CHAPTER 3

RESEARCH METHODOLOGY

The methodology of the research is start from Molecular Structure Construction, after that optimize the monomer molecules. The AutoDock program is used to find the possible conformation of the inclusion complex by setting the fixed host and movable guest. After the possible conformations were found, the optimization of the possible inclusion complex begins. Next, we calculated the complexation energy. Computer-aided molecular modeling is used to find out binding interaction and thermodynamics properties of interested complex system. Then, the molecular dynamics simulation was used to confirm the results.

3.1 Molecular Structure Construction

The molecular structure of plumbagin (guest) compound molecule structures was constructed by GaussView 6.0 program. All of Cyclodextrin molecular structures (host) obtained from Cambridge Crystallographic data file (CCDF) (Lichtenthaler & Immel, 1996). The structure including BCD, MBCD and HPBCD were downloaded as follows:

- BCD, BCDEXD03 or β -Cyclodextrin hydrate clathrate (Steiner & Koellner, 1994);
- MBCD, BOYFOK04 or heptakis (2,6-Di-O-methyl)- β -cyclodextrin pentadecahydrate (Aree et al., 2000);
- HPBCD, KOYYUS or 2-O-((S)-2-Hydroxypropyl)- β -cyclodextrin hydrate (Harata, Rao, Pitha, Fukunaga, & Uekama, 1991).

Hydrogen atoms were added into the structures, and then fully optimized by the semi-empirical quantum mechanical PM3, PM6 and PM7 methods. The polarizable continuum model (PCM) was used to model solvation effects for water as the solvent (Tomasi, Mennucci, & Cammi, 2005).

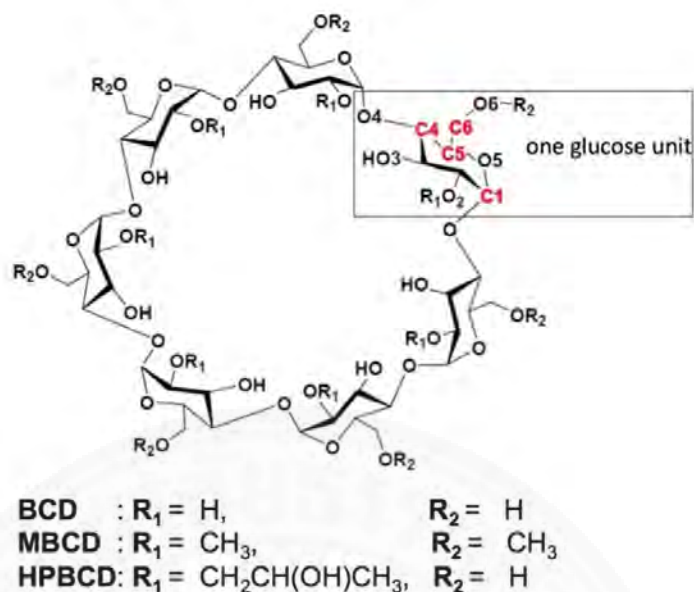


Figure 3.1 Schematic representations of glucose unit and atomic numbering of BCD, MBCD and HPBCD. All R_1 and R_2 are substituted by methyl groups on all of the glucose units in MBCD. In HPBCD, only the hydroxyl group at the R_1 position of one glucose unit is substituted

3.2 Molecular Docking Simulations

AutoDock 4.2.6 with the Lamarckian genetic algorithm was used to generate the possible conformations of plumbagin/BCDs inclusion complexes. AutoDock calculations were performed in four steps: (1) preparation of coordinate files using AutoDockTools, (2) pre-calculation of atomic affinities using AutoGrid, (3) docking of ligands using AutoDock, and (4) analysis of results using AutoDockTools.

The first step was to prepare the guest (plumbagin) and host (BCDs) coordinate files to include the information needed by AutoGrid and AutoDock. The non-polar hydrogen atoms were deleted and their charges were merged with the carbon atoms. The atom types were assigned, defining hydrogen bond acceptors and donors and aromatic and aliphatic carbon atoms. The rotatable bonds of the guests were defined while the hosts were kept fixed. AutoGrid was used to calculate the grid maps, one for each atom type present in the guest being docked. The systems were investigated in a three-dimensional volume divided into many small grid boxes with a grid spacing of 0.375 Å.

The grid center of the boxes was set at the center of the host molecules. The box has

$x \times y \times z$ dimensions of $14.25 \text{ \AA} \times 14.25 \text{ \AA} \times 7.50 \text{ \AA}$, $15.75 \text{ \AA} \times 14.25 \text{ \AA} \times 9.75 \text{ \AA}$ and $18.75 \text{ \AA} \times 14.25 \text{ \AA} \times 9.00 \text{ \AA}$ for BCD, MBCD, and HPBCD, respectively. The Lamarckian genetic algorithm was used to calculate the conformational states of a flexible guest, using the grid maps generated by AutoGrid to evaluate the interaction at each point in the docking simulation. One hundred docking calculations were performed on each guest–host complex. The results were clustered to identify similar conformations based on all-atom root mean square deviation within 2 \AA . At the end of molecular docking calculations, AutoDockTools was used to perform a cluster analysis of the different docked conformations. The lowest energy representative docked conformation from molecular docking was selected for further full geometry optimization.

3.3 Complexation Energy Calculation

The selected docked conformation of plumbagin/BCD inclusion complexes was then fully geometry optimized by the PM3, PM6 and PM7 methods. All atoms were allowed to move freely in an aqueous environment. The most stable conformation of the plumbagin/BCD, plumbagin/MBCD, and plumbagin/HPBCD inclusion complexes were selected by considering the complexation energy (ΔE) as being the difference between the heat of formation of the complex and the heat of formation of the involved free molecules

$$\Delta E = E_{\text{complex}} - (E_{\text{host}} + E_{\text{guest}}) \quad (3.1)$$

where E_{complex} is the inclusion complex energy between host and guest; E_{guest} is the energy of the guest molecule; and E_{host} is the energy of the host or BCD and its two derivatives, MBCD and HPBCD. The inclusion complex with the lowest energy or negative value presents the most stable inclusion complex. On the other hand, the positive value shows that they are unfavorable to form the inclusion complexes.

3.4 Molecular Dynamics (MD) Simulation

The AMBER18 program with Glycam06 force fields was used for MD simulations. The inclusion complex systems from molecular docking are solvated with a periodic truncated octahedral box of TIP3P water molecules. Energy minimization was performed with 1000 cycles of steepest descent, followed by 1000 cycles of conjugate gradient, to reduce steric conflicts between water molecules and the complex. Then, the solvent equilibration was performed. The system was gradually heated from 0 to 273.15 K over 20 ps with the volume held constant. After heating for 20 ps, the system had a temperature of 273.15 K and a density of 1 g/cm³, i.e., the experimental density of water. Then, the MD simulations were performed for 35 ns at 298.15 K and 1 atm (isothermal–isobaric ensemble, NPT) with 2 fs time steps. The system properties that can be extracted from the data output files during MD simulations are energies, temperatures, pressures, volumes, densities, and structural RMSDs (root mean square deviations). In addition, free BE estimation by the MM/GBSA method has been used to calculate the BE between each host and guest.

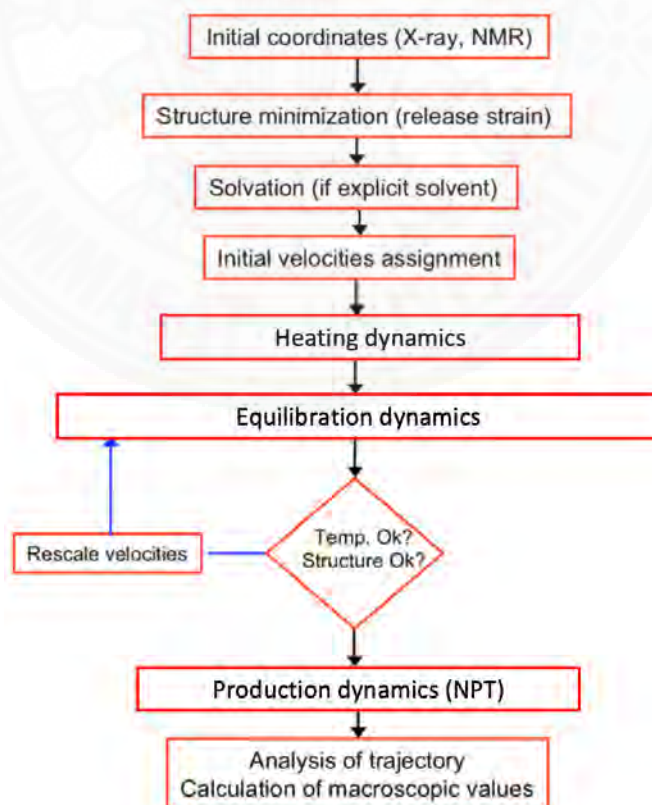


Figure 3.2 Flowchart of the molecular dynamics simulation modified from (Case, 2018)

CHAPTER 4

RESULTS AND DISCUSSION

In this chapter, the results are presented following the procedure in the research methodology section. First, the results will start from Molecular Docking Calculation, Complexation Energy Calculation and Molecular Dynamics (MD) Simulation. Then, all results are discussed in this section.

4.1 Molecular Docking Calculation

Molecular docking was used to calculate the possibility of binding between a plumbagin molecule complex with each BCD by fixing the host structure and allowing the guest to be flexible in the specified grid box. The calculations indicated two possible conformations of the 1:1 guest:host ratio for all systems, as shown in Tables 4.1 to 4.3. In conformation-I, the hydroxyl phenolic group of plumbagin was placed in the BCD cavity near the narrow-side of the host molecule. In the other model, conformation-II, the methyl quinone group of plumbagin was placed in the BCD cavity near the narrow-side of the host molecule, as illustrated in Figure 4.1.

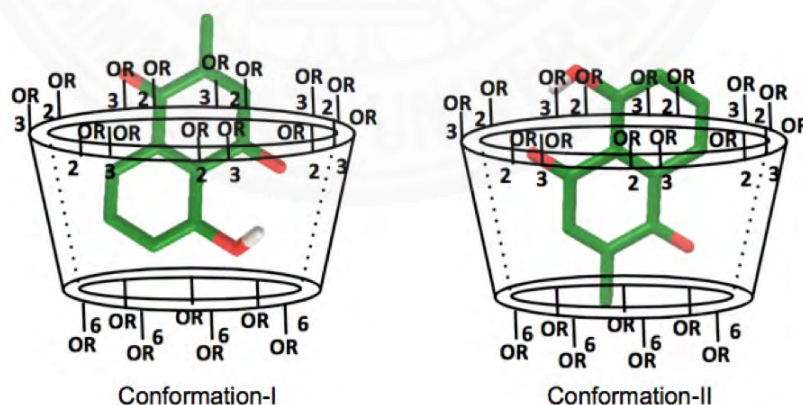


Figure 4.1 Schematic representation of two conformations of the inclusion complex. The secondary hydroxyl groups are at the C2 and C3 positions of the BCD, which are located on the wide-side of the truncated cone. The primary hydroxyl group is at the C6 position of the BCD, which is located at the narrow-side of the truncated cone.

For PM3 results plumbagin/BCD and plumbagin/HPBCD prefer conformation-I, on the other hand, plumbagin/MBCD shows the conformation-II was favorable. The molecular docking results, which obtained from PM6 and PM7 minimized starting geometries, provide the same information for the favorable inclusion complexes conformation. Conformation-I was the most energetically favored for plumbagin/BCD and plumbagin/MBCD inclusion complexes while plumbagin/HPBCD preferred the conformation-II. However, the rigidity of the host molecule in the docking calculations was not realistic. Therefore, the semi-empirical PM3, PM6 and PM7 methods in the aqueous phase using polarizable continuum computations, were used to further investigate the molecular interactions of plumbagin with three different BCD hosts.

Table 4.1 The lowest and the average values of free energy of binding (ΔG) of plumbagin/BCDs inclusion complexes and the number of conformations in a cluster (frequency) obtained from molecular docking calculations at 298.15 K. The starting geometry of the host and guest molecules were optimized by the PM3 method.

Guest/Host	Cluster	Conformation	Frequency (%)	ΔG (kcal/mol)	
				Lowest	Average
plumbagin/BCD	1	I	33	-5.86	-5.83
	2	I	61	-5.82	-5.81
	3	II	6	-5.65	-5.64
plumbagin/MBCD	1	I	63	-5.74	-5.74
	2	II	37	-5.74	-5.73
plumbagin/HPBCD	1	I	100	-5.53	-5.50

Table 4.2 The lowest and the average values of free energy of binding (ΔG) of plumbagin/BCDs inclusion complexes and the number of conformations in a cluster (frequency) obtained from molecular docking simulations at 298.15 K. The starting geometry of the host and guest molecules were optimized by the PM6 method.

Guest/Host	Cluster	Conformation	Frequency (%)	ΔG (kcal/mol)	
				Lowest	Average
plumbagin/BCD	1	I	100	-6.21	-6.19
plumbagin/MBCD	1	I	85	-5.14	-5.13
	2	II	15	-5.03	-5.02
plumbagin/HPBCD	1	II	48	-5.76	-5.75
	2	I	2	-5.74	-5.73
	3	I	50	-5.72	-5.71

Table 4.3 The lowest and the average values of free energy of binding (ΔG) of plumbagin/BCDs inclusion complexes and the number of conformations in a cluster (frequency) obtained from molecular docking calculations at 298.15 K. The starting geometry of the host and guest molecules were optimized by the PM7 method.

Guest/Host	Cluster	Conformation	Frequency (%)	ΔG (kcal/mol)	
				Lowest	Average
plumbagin/BCD	1	I	61	-5.34	-5.26
	2	I	2	-5.24	-5.23
	3	II	24	-5.22	-5.21
	4	II	13	-5.20	-5.18
plumbagin/MBCD	1	I	100	-5.12	-5.12
plumbagin/HPBCD	1	II	100	-5.89	-5.87

4.2 Complexation Energy Calculations

An inclusion complex of plumbagin with each of the BCD systems from docking simulations was generated. Both conformation-I and conformation-II, were then fully optimized by the PM3, PM6 and PM7 methods, which provide free motions for host and guest molecules in an aqueous environment. From PM3, PM6 and PM7 results, the heat of formation of the minimized structure of the complex was always lower than that of the sum of the heat of formation of the isolated guest and host molecules indicating the formation of a favorable complex in all models. The complexation energy (ΔE), according to Equation (3.1), is also shown in Table 4.4. The more negative the value of the complexation energy, the more favorable the pathway of inclusion-complex formation. Table 3 shows the favorable formation of a 1:1 guest:host ratio of plumbagin with three type of BCD in both possible conformations.

The magnitudes of complexation energy (ΔE) from PM7 (-41.41 to -30.10 kcal/mol) were considerably larger than PM6 (-12.78 to -5.70 kcal/mol), and PM3 (-4.30 to 1.85 kcal/mol). The PM7 method includes the description of the dispersion interaction and hydrogen bonding (James J.P. Stewart, 2013) in the parameterization, and thus, should be suitable for the description of noncovalent interactions in plumbagin/BCD complexes. For the previous study in DFT calculations in these inclusion complexes (Srihakulung, 2018), the results of B3LYP principally provide the positive value in complexation energy (-4.86 to 3.11 kcal/mol), while other functionals

(five dispersion-corrected functionals were assessed in this study: CAM-B3LYP, B3LYP-GD3, CAM-B3LYP-GD3, M06-2X, and M06-2X-GD3) illustrate the negative value from -33.23 to -1.25 kcal/mol. The conventional functionals such as the B3LYP functional are unable to describe the long-range or the intermolecular interaction precisely (Grimme, 2011). The DFT with CAM functionals can capture a further range of interaction from the higher fraction of HF. As a result, the complexation energy is larger than B3LYP (-3.94 to -1.25 kcal/mol). M06-2X is a high non-locality with a double amount of nonlocal exchange (global hybrid functional contains 54% HF exchange) (Zhao, Schultz, & Truhlar, 2006). The higher percentage of HF affects M06-2X to capture the long-range interaction part, resulting in the higher negative value of complexation energy in the range between -21.61 to -13.51 kcal/mol. The DFT with GD correction functional includes vdW interaction with default parameters for GGA-PBE functional which can capture the intermolecular interaction (Grimme, Antony, Ehrlich, & Krieg, 2010). For all B3LYP with DFT-GD3, the complexation energy is larger in the range from -33.23 to -25.46 kcal/mol. Comparing all calculations (both DFT and semiempirical), the PM7 method provides the lowest complexation energy. The difference in ΔE between the two conformations (conformation-I–conformation-II), is also presented in Table 4.4. The obtained results indicated that plumbagin/BCD inclusion complexes prefer conformation-I (BCD-I) in a water environment. For the inclusion complex formation of plumbagin with modified β -cyclodextrins (MBCD and HPBCD), both conformation-I and conformation-II are favorable.

The difference in ΔE between the two conformations (conformation-I–conformation-II), is also presented in Table 4.4. The obtained results indicated that plumbagin/BCD inclusion complexes prefer conformation-I (BCD-I) in a water environment. For the inclusion complex formation of plumbagin with modified β -cyclodextrins (MBCD and HPBCD), both conformation-I and conformation-II are favorable.

Table 4.4 Heat of formation energy (E) and complexation energy (ΔE) in kcal/mol of the minimized inclusion complexes structures from PM6 and PM7 methods

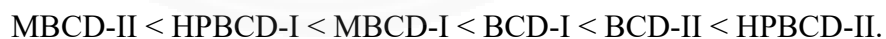
	PM3		PM6		PM7	
	E	ΔE	E	ΔE	E	ΔE
Isolated molecule						
Plumbagin	-83.28		-84.56		-87.09	
BCD	-1490.47		-1614.25		-1648.53	
MBCD	-1394.45		-1543.64		-1573.87	
HPBCD	-1532.94		-1659.94		-1701.90	
Inclusion Complex						
BCD-I	-1571.90	1.85	-1704.99	-6.18	-1768.09	-32.47
BCD-II	-1575.89	-2.14	-1704.97	-6.15	-1765.72	-30.10
BCD-I-BCD-II		2.68		-0.03		-2.37
MBCD-I	-1482.03	-4.30	-1636.23	-8.03	-1702.37	-41.41
MBCD-II	-1481.78	-4.05	-1640.97	-12.78	-1699.12	-38.17
MBCD-I-MBCD-II		-0.25		4.75		-3.24
HPBCD-I	-1620.43	-4.20	-1753.57	-9.08	-1820.19	-31.21
HPBCD-II	-1616.01	0.21	-1750.20	-5.70	-1829.73	-40.75
HPBCD-I-HPBCD-II		-4.41		-3.38		9.54

From Figure 4.2, all of the calculations illustrate negative values in the complexation energy, which means that all of the conformations prefer to form the inclusion complex. The results from PM3, PM6 and PM7 computations are presented respectively.

Firstly, PM3 are in the following order:



For PM6 result, the complexation energy are in the following order:



For PM7 are in the following order:



PM3 and PM6 provide the same range of binding energy. The PM7 method can improve some properties such as the heats of formation (height of the reaction barriers for reactions) and include them into dispersion interaction and hydrogen bonding in the parametrization, which should be suitable for the description of non-covalent interactions. On the other hand, there are some limitations of this method including large error for the non-covalent interaction energy. Three methods illustrate the

different candidate conformation. PM3 shows MBCD-I, while PM6 represents MBCD-II, and PM7 suggests that MBCD-I is the candidate conformation. To specify the force, the factor affecting the binding energy of each conformation, the studies consider the interactions between host and guest of the complexation. The intermolecular interactions between host-guest include, hydrogen bond interaction, C-H bond interaction and hydrophobic force. The number of bonds of each methods are counted and shown in Table 4.5.

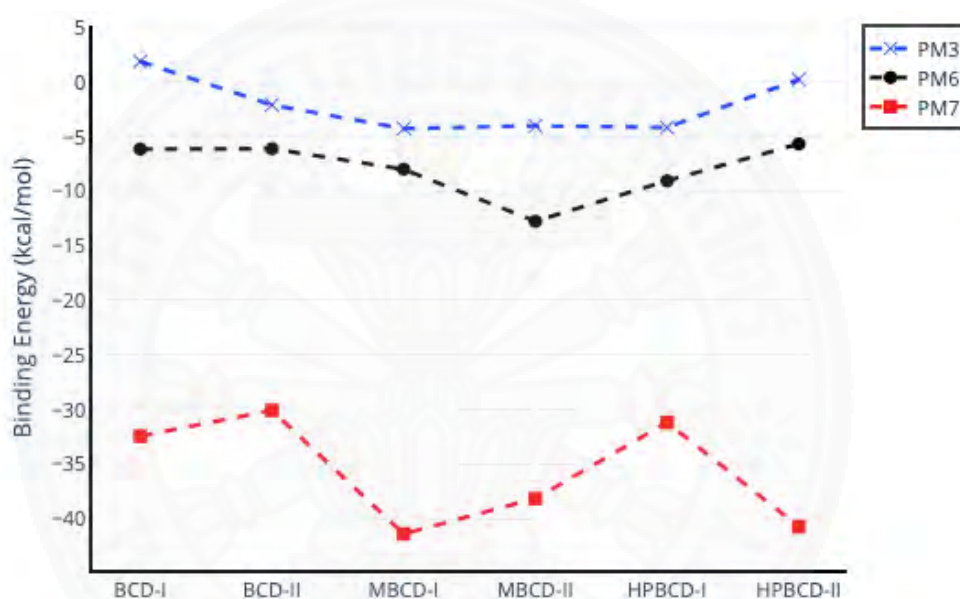


Figure 4.2 The complexation energy of six conformations by semi-empirical methods (PCM calculation), including PM3, PM6 and PM7.

Table 4.5 presents the distances of the intermolecular hydrogen bonds, which are found in PM3, PM6 and PM7 minimized inclusion complex structures. Three types of hydrogen bonds were established. The first one, which is often found in inclusion complex systems, is between an ether-like anomeric oxygen atom of the host molecule and a hydrogen atom of plumbagin's hydroxyl group ($O4_{(host)} \cdots H_{(OH-PL)}$). The second one, found only in plumbagin/BCD complexes, is from an oxygen atom of plumbagin's carbonyl group and the hydrogen atom of the secondary hydroxyl group at O3 of BCD-I ($O_{(CO-PL)} \cdots H_{(O3H-BCD)}$) and the primary hydroxyl at O6 of BCD-II ($O_{(CO-PL)} \cdots H_{(O6H-BCD)}$). The third one, is found only in HPBCD-II, between an oxygen

Table 4.5 Distance of hydrogen bonds between plumbagin (PL) and three different types of cyclodextrins (BCD, MBCD, and HPBCD) molecules, obtained from PM3, PM6 and PM7 minimized inclusion complex structures

			Distance (Å)
PM3	BCD-I	O _{6(BCD)} ... H _(OH-PL)	1.82
		O _(CO-PL) ... H _(C3H-BCD)	1.89
	BCD-II	O _(CO-PL) ... H _(C3H-BCD)	1.90
		O _(CO-PL) ... H _(C2H-BCD)	2.60
	MBCD-II	O _(CO-PL) ... H _(C3H-MBCD)	1.86
	HPBCD-I	O _{6(HPBCD)} ... H _(OH-PL)	2.78
		O _(CO-PL) ... H _(C3H-HPBCD)	1.84
	HPBCD-II	O _(CO-PL) ... H _(C5H-HPBCD)	1.85
		O _(CO-PL) ... H _(C5H-HPBCD)	2.88
		O _{6(BCD)} ... H _(OH-PL)	2.93
PM6	BCD-I	O _{4(BCD)} ... H _(OH-PL)	2.05
		O _(CO-PL) ... H _(O3H-BCD)	2.93
	BCD-II	O _{4(BCD)} ... H _(OH-PL)	1.92
		O _(CO-PL) ... H _(O6H-BCD)	2.95
	MBCD-I	O _{4(MBCD)} ... H _(OH-PL)	2.11
	HPBCD-I	O _{4(HPBCD)_n} ... H _(OH-PL)	2.20
		O _{4(HPBCD)_{n+1}} ... H _(OH-PL)	2.97
	HPBCD-II	O _{4(HPBCD)} ... H _(OH-PL)	3.07
		O _(OH-PL) ... H _(O2H-HPBCD)	2.09
		O _{4(BCD)_n} ... H _(OH-PL)	2.60
PM7	BCD-II	O _{4(BCD)_{n+1}} ... H _(OH-PL)	2.60
		O _{4(BCD)_{n+1}} ... H _(OH-PL)	2.60
	HPBCD-I	O _{4(HPBCD)} ... H _(OH-PL)	2.46
	HPBCD-II	O _{4(HPBCD)} ... H _(OH-PL)	2.62

atom of plumbagin's hydroxyl group and the hydrogen atom of the secondary hydroxyl at O2 of HPBCD (O_(OH-PL) ... H_(O2H-HPBCD)). The molecular interactions of each host–guest system in an aqueous environment are further discussed below.

4.2.1 Plumbagin/BCD Inclusion Complex

Two conformations of a plumbagin/BCD inclusion complex can be formed in an aqueous environment, as shown in Figure 4.3. The intermolecular hydrogen bonds between plumbagin and BCD are depicted in Figure 4.4. BCD-I has 2.68, 0.03 and 2.37 kcal/mol lower complexation energies from the PM3, PM6 and PM7 methods,

respectively, than BCD-II. The minimized plumbagin/BCD conformations obtained from the two methods were similar. However, in BCD-I from the PM7 computation, the plumbagin molecule dipped deeper into the BCD cavity than the optimized structures at the PM3 and PM6 methods. This occurred due to the hydrogen bond between the oxygen atom of plumbagin's carbonyl group and the hydrogen atom of the secondary hydroxyl group at O3 of BCD-I ($O_{(CO-PL)} \cdots H_{(O3H-BCD)}$), as shown in Figure 4.4(a) and 4.4(c).

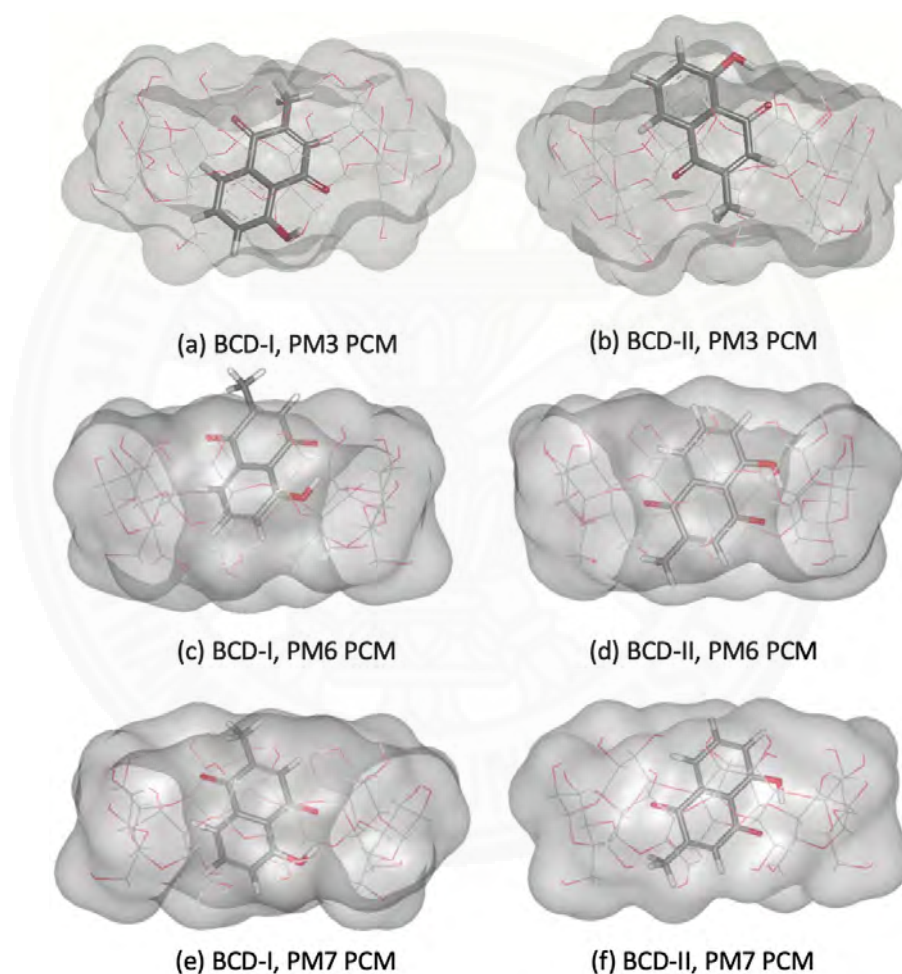


Figure 4.3 Energy-minimized structures of the 1:1 plumbagin/BCD complexes in an aqueous environment using polarizable continuum model (PCM). BCD presented as a line model with a surface, with a probe radius of 1.4 Å. The plumbagin molecule is presented as a stick model. (a) plumbagin/BCD conformation-I obtained from PM3 method, (b) plumbagin/BCD conformation-II obtained from PM3 method, (c) plumbagin/BCD conformation-I obtained from PM6 method and (d) plumbagin/BCD conformation-II obtained from PM6 method, (e) plumbagin/BCD conformation-I obtained from PM7 method and (f) plumbagin/BCD conformation-II obtained from PM7 method.

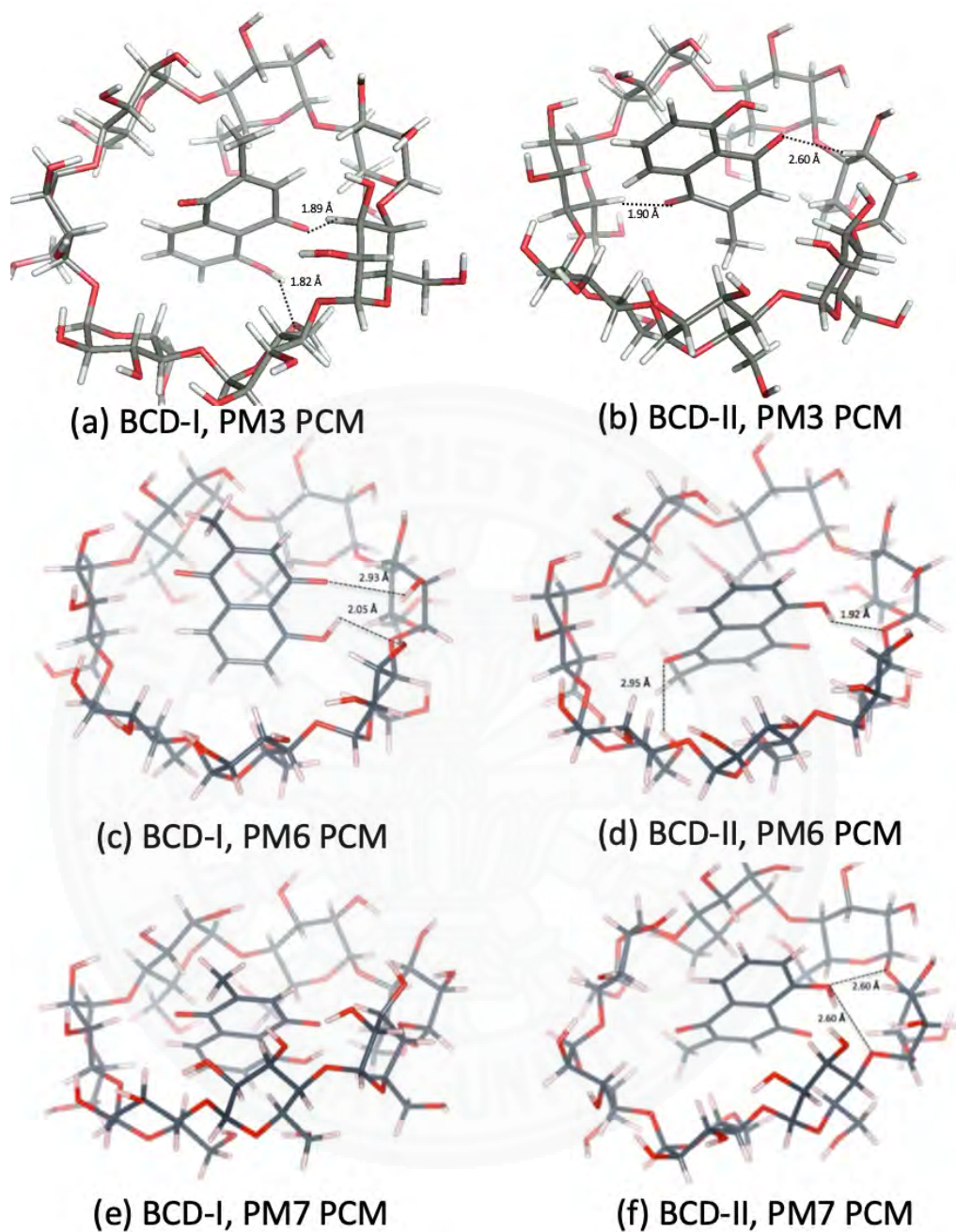


Figure 4.4 Hydrogen bonds in 1:1 plumbagin/BCD complexes. (a) plumbagin/BCD conformation-I obtained from PM3 method, (b) plumbagin/BCD conformation-II obtained from PM3 method, (c) plumbagin/BCD conformation-I obtained from PM6 method, (d) plumbagin/BCD conformation-II obtained from PM6 method, (e) plumbagin/BCD conformation-I obtained from PM7 method and (f) plumbagin/BCD conformation-II obtained from PM7 method.

4.2.2 Plumbagin/MBCD Inclusion Complex

The plumbagin molecule is located near the wide-side of the MBCD molecule in all complex conformations, as shown in Figures 4.5 and 4.6. These occurred due to the presence of methyl groups at the primary hydroxyl group of all glucose units (C6 position), condensing the cavity near the narrow-side of MBCD. In MBCD-I, without the steric hindrance from the guest molecule, all seven methoxy groups at the C6 position can be accommodated. After insertion of a plumbagin molecule in MBCD-II, two of the methoxy groups at the C6 position of MBCD move away from the cavity due to the presence of the methyl group of the plumbagin molecule, located at the narrow-side of MBCD, as seen in Figure 4.6, (d) and (f). According to the steric and electronic hindrances, plumbagin should enter into MBCD at the wide side to form the inclusion complexes MBCD-I and MBCD-II. The plumbagin/MBCD inclusion complex structures are very complicated. Using the same initial starting geometry, the energy-minimized conformations obtained from the PM3, PM6 and PM7 methods were altered.

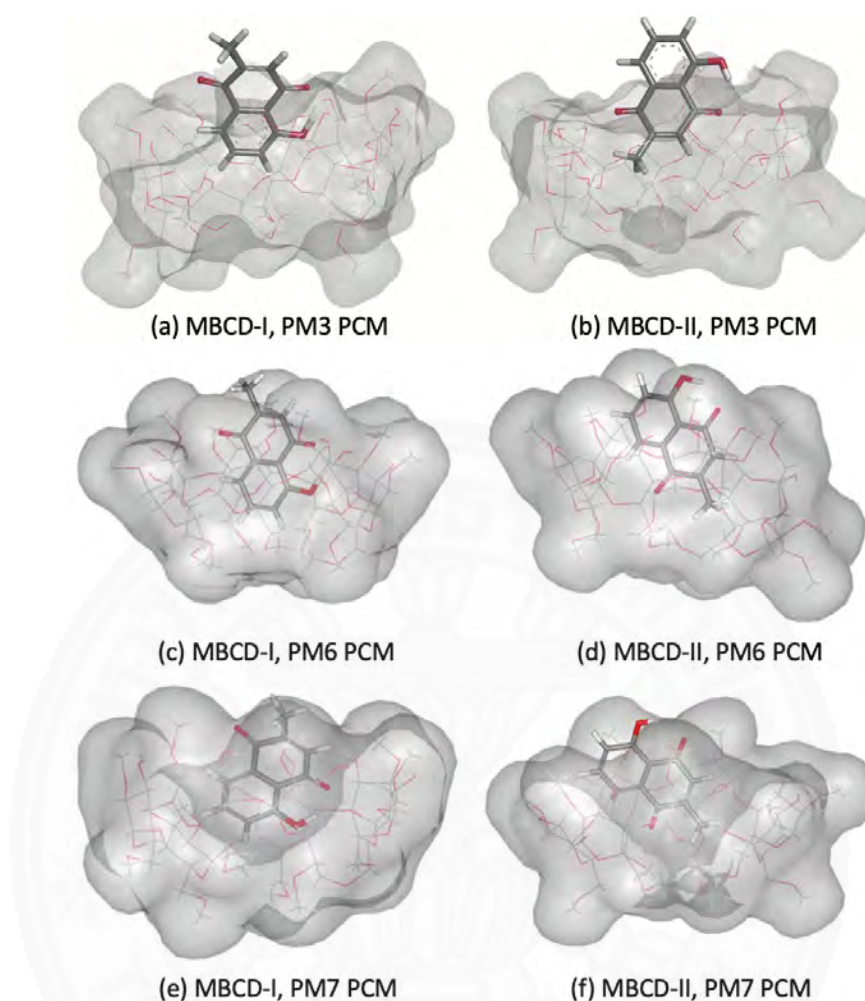


Figure 4.5 Energy-minimized structure of the 1:1 plumbagin/MBCD complexes in an aqueous environment using polarizable continuum model (PCM). MBCD is presented as a line model with a surface, with a probe radius of 1.4 Å. The plumbagin molecule is presented as a stick model. (a) plumbagin/MBCD conformation-I obtained from PM3 method, (b) plumbagin/MBCD conformation-II obtained from PM3 method, (c) plumbagin/MBCD conformation-I obtained from PM6 method and (d) plumbagin/MBCD conformation-II obtained from PM6 method, (e) plumbagin/MBCD conformation-I obtained from PM7 method and (f) plumbagin/MBCD conformation-II obtained from PM7 method.

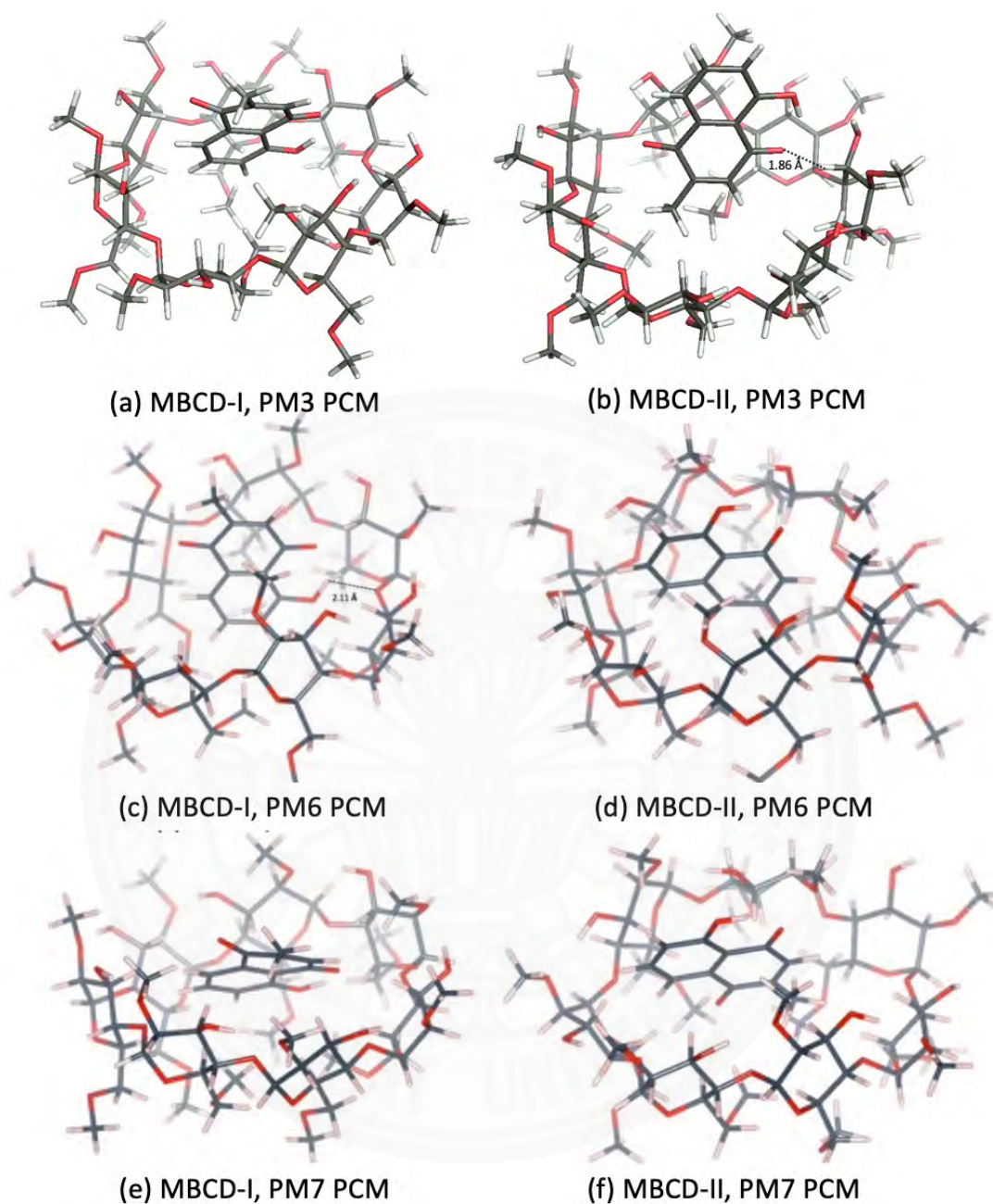


Figure 4.6 Hydrogen bonds in 1:1 plumbagin/MBCD complexes. (a) plumbagin/MBCD conformation-I obtained from PM3 method, (b) plumbagin/MBCD conformation-II obtained from PM3 method, (c) plumbagin/MBCD conformation-I obtained from PM6 method, (d) plumbagin/MBCD conformation-II obtained from PM6 method, (e) plumbagin/MBCD conformation-I obtained from PM7 method and (f) plumbagin/MBCD conformation-II obtained from PM7 method.

4.2.3 Plumbagin/HPBCD Inclusion Complex

The inclusion complex of plumbagin and HPBCD in conformation-I and conformation-II were stabilized in a water environment, as shown in Figures 4.7 and 4.8. The presence of the hydroxypropyl group at the C2 position on a glucose unit in HPBCD enlarges the width of the wide-side. The energy-minimized structures of HPBCD-I from the PM3, PM6 and PM7 methods were similar. The hydroxypropyl group of HPBCD lined up in the parallel direction with the methyl group of the plumbagin molecule. The guest molecule is located inside the HPBCD's cavity with an H-bond between the hydrogen atom of plumbagin's hydroxy group and the ether-like anomeric oxygen atom of HPBCD.

PM3, PM6 and PM7 computations yield different HPBCD-II energy-minimized structures in a water environment. In HPBCD-II, for the PM6 computation, the guest molecule is located near the wide-side of HPBCD (Figure 4.6d), due to the H-bond which formed between the hydroxyl group of plumbagin and the secondary hydroxyl group at O2 of HPBCD ($O_{(OH-PL)} \cdots H_{(O2H-HPBCD)}$), as mentioned in Table 4.5 and depicted in Figure 4.8d. Therefore, the guest molecule could not go deeper inside the HPBCD's cavity, yielding HPBCD-I as the preferable complex with a lower complexation energy (4.41 kcal/mol) than HPBCD-II in the PM3 calculations. In the PM7 calculations, HPBCD-II was more favorable with a lower complexation energy (9.54 kcal/mol) than HPBCD-I. The methyl part of the hydroxypropyl group substituent falls into the HPBCD's cavity and pushes the plumbagin molecule deeper inside the cavity due to the hydrophobic interaction.

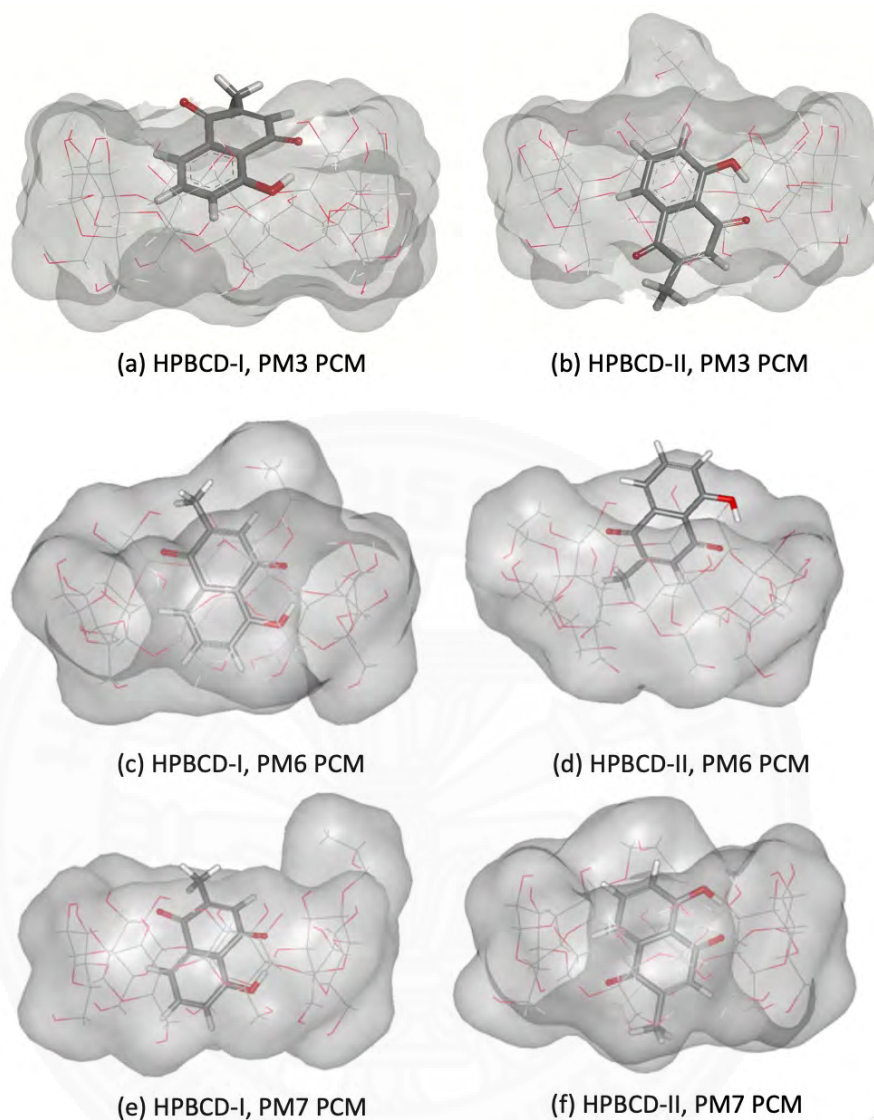


Figure 4.7 Energy-minimized structures of the 1:1 plumbagin/HPBCD complexes in an aqueous environment using polarizable continuum model (PCM). HPBCD presented as a line model with a surface, with a probe radius of 1.4 Å. The plumbagin molecule is presented as a stick model. (a) plumbagin/HPBCD conformation-I obtained from PM3 method, (b) plumbagin/BCD conformation-II obtained from PM3 method, (c) plumbagin/HPBCD conformation-I obtained from PM6 method and (d) plumbagin/HPBCD conformation-II obtained from PM6 method, (e) plumbagin/HPBCD conformation-I obtained from PM7 method and (f) plumbagin/HPBCD conformation-II obtained from PM7 method.

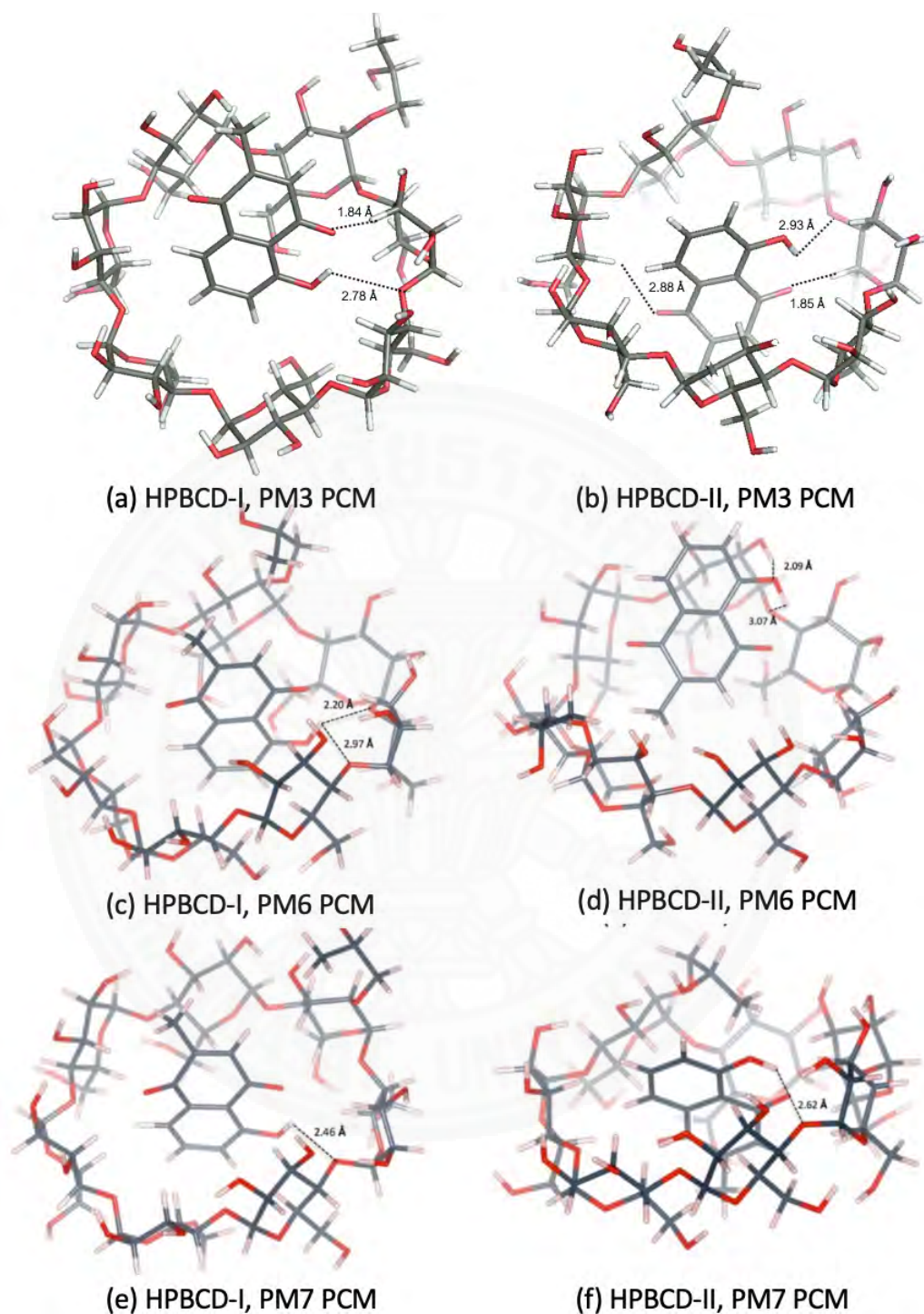


Figure 4.8 Hydrogen bonds in 1:1 plumbagin/HPBCD complexes. (a) plumbagin/MBCD conformation-I obtained from PM3 method, (b) plumbagin/HPBCD conformation-II obtained from PM3 method, (c) plumbagin/HPBCD conformation-I obtained from PM6 method, (d) plumbagin/HPBCD conformation-II obtained from PM6 method, (e) plumbagin/HPBCD conformation-I obtained from PM7 method and (f) plumbagin/HPBCD conformation-II obtained from PM7 method.

4.3 Molecular Dynamics (MD) Simulation

The structures of inclusion complex between BCD and its derivative with plumbagin in aqueous solution were simulated by MD simulations using AMBER18 software package. BCD molecule were treated by Glycam06 carbohydrate force field. The structures of complexes were optimized by PM7 level of theory using Gaussian 16 program. The inclusion complexes were solvated using simple-point charge (SPC) water molecule in a periodic truncated octahedron water box, which had a minimize distance from the system surface of 12 Å. The octahedron periodic water roughly consisted of 1,400 – 1,900 water molecules.

The SHAKE algorithm was utilized to constrain all covalent bonds involving hydrogen atoms. The temperature increases from 0 K to 298.15 K over a period of 100 ps. This research considered at this temperature and with 1 atm for 50 ns. A periodic boundary condition with isobaric-isothermal (NPT) ensemble was applied for all simulations. The simulation time step was set at 2 fs and trajectories were collected every 2 ps for analysis. The MD results were considered into two parts, for the first part, the research consider energy and thermodynamic properties of complex. Finally, RMSD and take suitable interval for calculating free binding energy between host and guest.

The results of MD calculations will be grouped into 3 parts, following each molecules. The system stability (RMSD), the distance between the center of mass of the plumbagin molecule and CDs, and host-guest binding free energy determined by MM-GBSA were described in each section. The calculation measures the deviation of the target set of coordinates to the reference set of coordinates. To gain more information about the dynamic stability of each inclusion complex, BCD-I, BCD-II, MBCD-I, MBCD-II, HPBCD-I, and HPBCD-II, extensive simulations were computed and visualized. The experiment can assist in observing the stability of the system during initial setting conditions. For more information toward the dynamic stability of inclusion complexes (BCD, MBCD, and HPBCD with Plumbagin), 1D-RMSD of each MD system relative to the initial structure versus simulation time was calculated and shown in Figure 4.9, which expresses RMSD plots for inclusion complexes (black), CDs (blue) and plumbagin (red) with the simulation time.

From Figure 4.9, the averaged RMSDs of all inclusion complexes are in the same range of 1.0 to 4.0 Å. The RMSDs of plumbagin in any inclusion complex are similar in the range of 0.2 to 0.8 Å. However, the difference in RMSD fluctuations of each complex arises from other factors, such as the structure of CDs and dynamical properties of plumbagin during binding inside the CDs molecules.

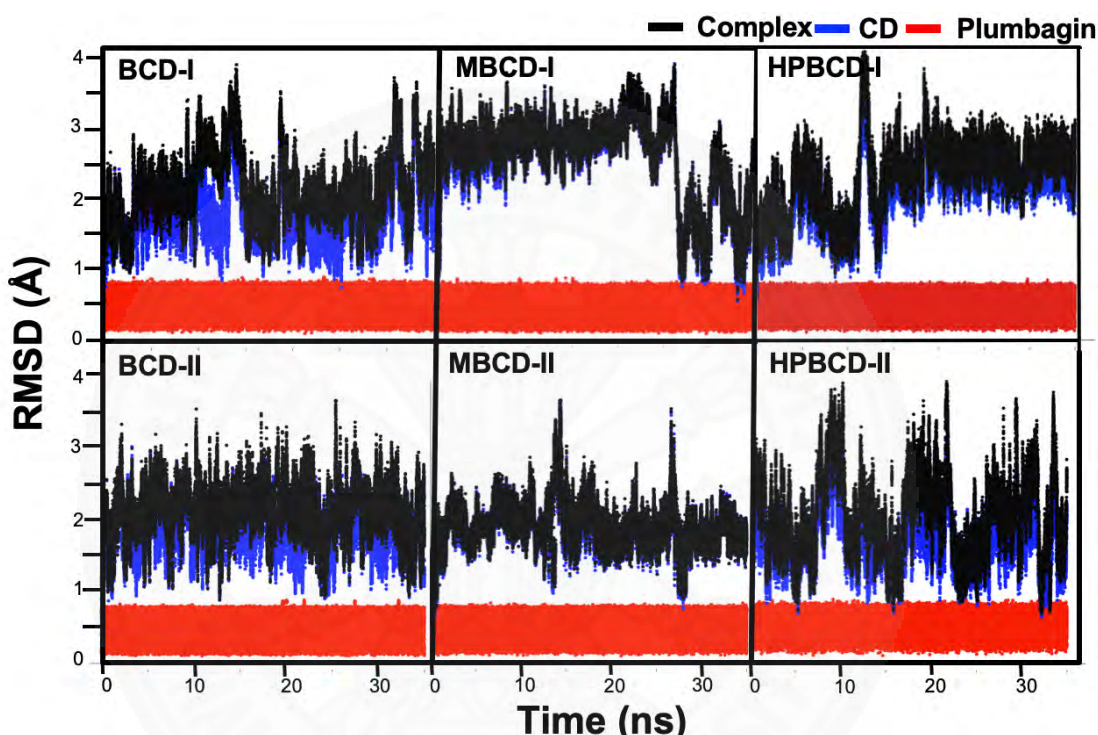


Figure 4.9 RMSD plots of all six inclusion complexes, where the inclusion complexes, CDs and plumbagin are highlight by black, blue, and red, respectively.

Figure 4.10 presents the plumbagin behavior inside three different BCDs cavities. The distance between the center of mass of plumbagin and the center of mass of BCDs are defined. The substitute groups of two derivatives are not taken into consideration. The horizontal dashed line indicates the positions at -3.95 Å and 3.95 Å on the y-axis approximately. The negative and positive values represent the orientation of the plumbagin molecule below or above the center of mass of the CDs molecules.

Recommended methods to estimate the binding of small ligands and other biological macromolecules include molecular mechanics Poisson-Boltzmann/Generalized Born surface area continuum solvation (MM/PBSA and MM/GBSA). Based on receptor-ligand complex MD simulations, both methods are

standard for computational application and accuracy for strict alchemical and empirical scoring, thus applying to various systems with differing achievements. For BCDs and Plumbagin binding calculation, the experiment examines 5,000 frames (1 frame equals 1 ps) during 15 to 20 ns.

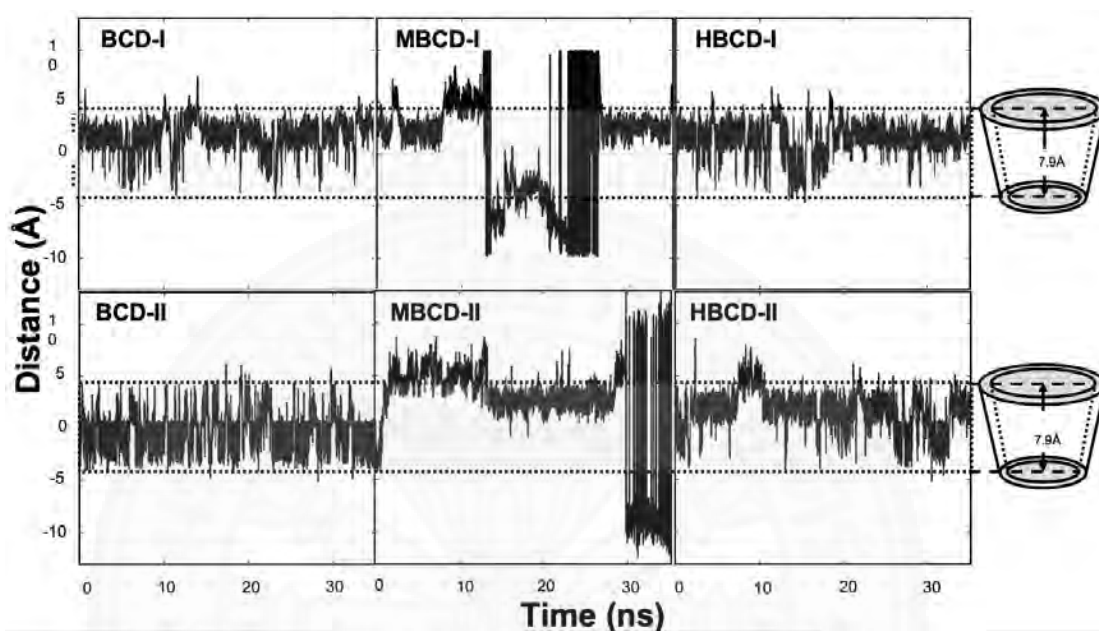


Figure 4.10 Distance between the center of mass of plumbagin with BCD and two derivatives.

The MM/GBSA approaches are used to predict the free energy of binding for the host-guest inclusion complex as shown in Table 1. Basically, the differences in free energy between the complex plus host and guest molecule are used to determine the binding free energy of the inclusion complex. The energetic components consist of the gas phase energy (ΔE_{MM}) increase by the summation between electrostatic (ΔE_{ele}) and van der Waals (ΔE_{vdW}) energies, the free energy of solvation (ΔG_{solv}) and entropy contribution ($T\Delta S$). Since the structure and dynamical behavior of Plumbagin bind with CDs cavity, the binding energy can be predicted by MM-GBSA methods for all complexes.

From Table 4.6, the negative binding free energy of all of the inclusion complexes is in the range of -14.61 to -11.80 kcal/mol and the binding energy results clearly observe that this is the favorable host and guest complex in pure water. The binding free energy estimated from MM/GBSA of plumbagin and BCDs inclusion

complexes is in the order of MBCD-II > MBCD-I > HPBCD-I > HPBCD-II > BCD-II > BCD-I. MBCD-II provides the highest negative binding energy. Due to the high lipophilicity (log P 3.04) of plumbagin (Pawar, Patel, Arulmozhi, & Bothiraja, 2016), thus some hydrogen bonds between host guest molecules were found, which is related to some contribution of the electronic interaction (ΔE_{ele} , which provides during the range of -5.09 to -2.68 kcal/mol). It is related to some contribution of the electronic interaction (ΔE_{ele} , which provides during the range of -5.09 to -2.68 kcal/mol). On the other hand, the main contribution of plumbagin inclusion complexes gains from the van der Waals interaction (ΔE_{vdw}), which in the range of -24.87 to -20.79 kcal/mol.

Table 4.6 The detail of binding free energies in kcal/mol with the energy components of Plumbagin/CDs inclusion complexes

Component	BCD-I	BCD-II	MBCD-I	MBCD-II	HPBCD-I	HPBCD-II
ΔE_{ele}	-2.70 ± 2.77	-2.69 ± 2.14	-3.96 ± 2.03	-3.75 ± 2.16	-5.09 ± 2.95	-2.68 ± 2.44
ΔE_{vdw}	-22.24 ± 2.79	-21.50 ± 2.69	-20.79 ± 4.50	-24.87 ± 2.32	-21.93 ± 3.01	-23.11 ± 2.45
ΔG_{Gas}	-24.94 ± 3.38	-24.19 ± 3.50	-24.75 ± 5.74	-28.62 ± 3.12	-27.02 ± 4.26	-25.79 ± 3.43
ΔG_{Sol}	12.87 ± 2.62	11.67 ± 2.20	8.47 ± 2.47	11.05 ± 2.05	13.61 ± 3.16	12.20 ± 2.47
$-T\Delta S$	-0.28	-0.46	-2.46	-2.96	-0.23	-2.99
$\Delta G_{\text{bind(Total)}}$	-12.08 ± 0.63	-13.22 ± 2.13	-16.28 ± 3.66	-17.57 ± 2.23	-13.41 ± 2.74	-13.60 ± 2.21
$\Delta G_{\text{bind(QM/GBSA)}}$	-11.80	-12.76	-13.82	-14.61	-13.18	-12.97

4.3.1 Plumbagin/BCD Inclusion Complex

For the BCD inclusion complex, the initial conformation after heating at 298.15 K and the final conformation after running molecular dynamics simulation for 35 ns are shown in Figure 4.11. The various number of water molecules are surrounded by the BCD inclusion complex molecules. A higher number of water molecules are located near the methyl group of plumbagin molecules. For the final conformation, the plumbagin is captured inside the BCD cavity. Therefore, the hydrogen bonds are formed around the wider rim of BCD, resulting in the BCD containing the cone shape. However, an

interesting point, the BCD-I conformation prefers to arrange as down orientation. Finally, the plumbagin molecule rotates 180 degrees as BCD-II conformation.

For RMSD calculation, in BCD inclusion complex, the averaged RMSDs were lower than two derivative inclusion complexes, due to the effect of substituents. The less fluctuation (in the range of 0.4 to 3.9 Å) are shown in Figure 4.9. For the distance analysis between the center of mass of plumbagin and BCD in Figure 4.10, the results of BCD inclusion complexes indicate that the plumbagin molecule is mainly located inside the BCD's cavity (the distance is between -5.2 Å to 5.7 Å). During some periods of the results point out that the plumbagin molecules float up to the wider rim of BCD. For binding free energy results from MM/GBSA calculation (during 15 to 20 ns), BCD-II provides lower binding free energy than BCD-I. The main binding free energies are from van der Waals interaction revealed in the lower energy (in the range of -20 kcal/mol), compared to electronic energy (in the range of -2.5 to -3.0 kcal/mol). However, the binding free energy results are related to the final conformation as previously mentioned, that is the plumbagin of BCD-I conformation finally is orient similar to the BCD-II conformation.

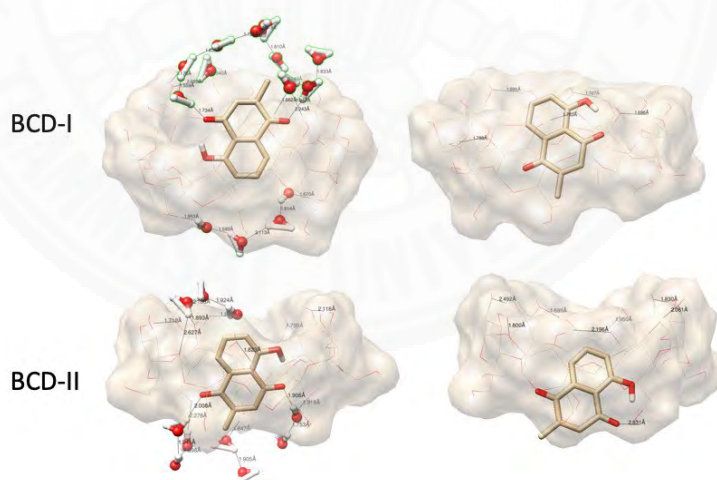


Figure 4.11 Two conformations illustration of BCD inclusion complexes: (left) bound form (right) intermediate along the releasing pathway.

4.3.2 Plumbagin/MBCD Inclusion Complex

conformations are visualized as in Figure 4.12. The MBCD molecules are distorted while the cone shapes disappear. Accordingly, the H-bonds at the wider rim are broken

from the substituted of the methyl groups. As a result, the plumbagin molecules fit to the host molecule. However, numbers of water molecules are surrounding the wider rim in MBCD-I and near the narrow rim in MBCD-II. There are some hydrogen bonds formed between water molecules with the methyl group and the oxygen atom at 1, 4-naphthoquinone. For the final conformation, all plumbagin of DMBCD inclusion complexes floats out from the host molecules. According to the results from the distance of the center of mass in Figure 4.10 indicates over ± 3.95 Å of the distance. However, the plumbagin molecule of MBCD-I can be captured and located inside the cavity from 25 to 35 ns. Otherwise, the plumbagin of MBCD-II has floated out after 28 ns. In Figure 4.9, MBCD inclusion complexes express the observably higher RMSD fluctuation within the range of 0.4 to 4.0 Å. Especially, two peaks at 13 ns and 27 ns are noticeably high RMSD fluctuation observed with MBCD-II. For MBCD-I, the starting of the RMSD has fluctuated, although after 25 ns the fluctuation decreases. In this part, the result is agreeable with the distance of the center of mass in Figure 4.10. For the MM/GBSA results from 15 to 20 ns, MBCD-II indicates the lower binding free energy than MBCD-I because the plumbagin molecule of DMBCD-I drop into the narrow side of the host molecule according to the distance of the center of mass results from Figure 4.10.

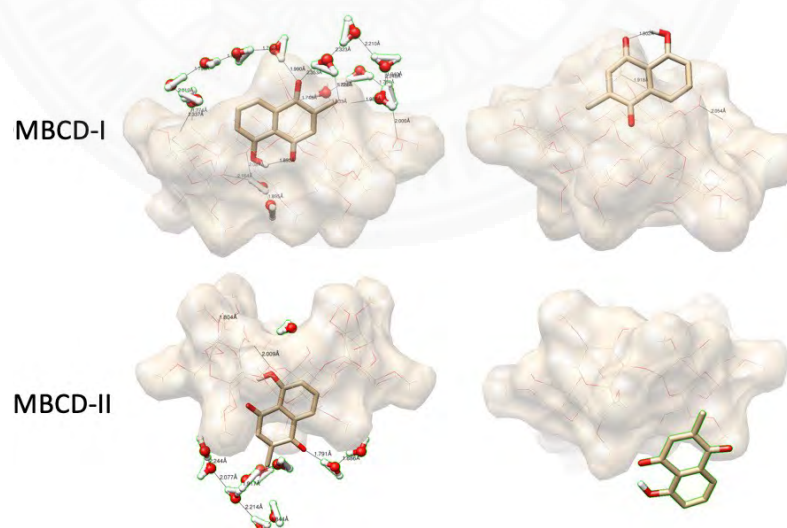


Figure 4.12 Two conformations illustration of MBCD inclusion complexes: (left) bound form (right) intermediate along the releasing pathway.

4.3.3 Plumbagin/HPBCD Inclusion Complex

Figure 4.13 shows the initial and final conformation of HPBCD inclusion complexes with plumbagin molecules. The initial conformations contain cone shape, despite the substitution by hydroxypropyl-group at the wider rim. As a result, the plumbagin molecule is captured inside the HPBCD's cavity. There are still some water molecules formed hydrogen bonds with the methyl group and the oxygen atom at 1, 4-naphthoquinone. For the final conformation results, two of the inclusions complexes point toward the same direction, thus the plumbagin molecule prefers to orient as the conformation- I.

For RMSD results of HPBCD (Figure 4.9), the result indicates similarity to the parent inclusion complexes. From the comparison of the CD structures of all inclusion complexes, the lower RMSDs suggest that the complexation with Plumbagin conducts to more rigid CD conformations. Furthermore, it is seen that the variance in RMSD fluctuations of the difference complexes evolved from the structure of host molecules and the different orientation and dynamical properties of guest molecule binding inside the host's cavity. For the distance of center of mass results (Figure 4.10), the plumbagin places inside the HPBCD's cavity almost the time. There is some peak data indicating that the plumbagin floats up near the wider rim of the host molecule. For the binding free energy results (Table 1), HPBCD-I provide the higher negative value of the energy during 15-20 ns. The results related to the final conformation suggest that the HPBCD prefers conformation-I than conformation-II.

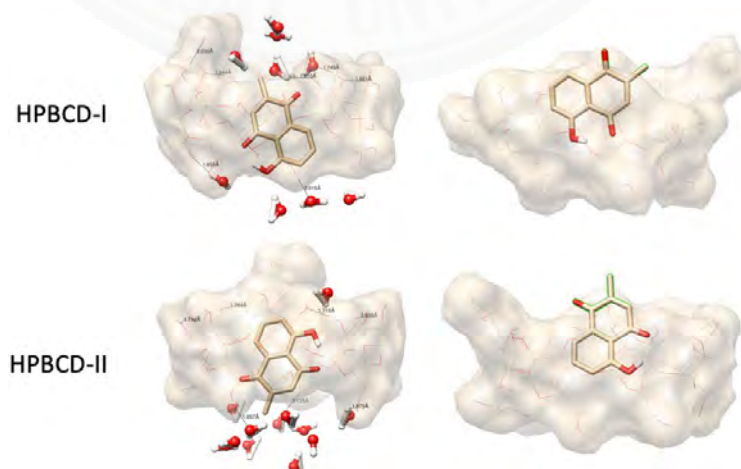


Figure 4.13 Two conformations illustration of HPBCD inclusion complexes: (left) bound form (right) intermediate along the releasing pathway.

In summary, the results of molecular dynamics simulations present the releasing direction of the plumbagin and dissociation rate of plumbagin and the CDs complexes. For the BCD inclusion complex, all of the hosts contain cup-shaped due to the hydrogen bond surrounding the wider rim of the truncated cone. As a result, Plumbagin is captured inside the cavity. For the releasing pathway for BCD-I, plumbagin seems to float out near to the wider rim of the host molecule. On the other hand, the guest molecule seems to sink and may get though at the narrow side for the BCD-II case. For the DMBCD inclusion complex, the cap seems to dis- tort, while the plumbagin is unable to maintain inside the deform cavity. As a result, this host is not suitable to encapsulate the plumbagin molecule. For HPBCD inclusion complexes, the host molecule contains some H- bond at the wider rim, which holds this molecule as the cone shape. One substitution of Hydroxypropyl group is unable to break the bond as fourteen of the methyl group. Besides, the plumbagin molecule prefers to orient as the conformation-I. As a result, the plumbagin of HPBCD-II flip horizontally to the opposite direction.

CHAPTER 5

CONCLUSIONS

Conclusions

The magnitudes of the complexation energies of each system obtained by the PM7 method are significantly larger than those obtained by the PM6 and PM3 method. The obtained results agree with the experimental data for a 1:1 guest:host ratio of plumbagin with BCD and HPBCD inclusion complexes. The present studies predict that by using MBCD and HPBCD to increase the solubility and reduce the cytotoxicity of the plumbagin compound, a 1:1 guest:host inclusion complex can be produced.

The molecular docking simulations indicated two possible conformations of the 1:1 guest:host ratio for all systems. In conformation-I, the hydroxyl phenolic group of plumbagin was placed in the BCD cavity near the narrow-side of the host molecule. In the other model, conformation-II, the methyl quinone group of plumbagin was placed in the BCD cavity near the narrow-side of the host molecule,

Our research studied two different models of solution, which include PCM and MD simulations. For PCM results which perform the computations with semiempirical method (PM3, PM6 and PM7), MBCD provide the lowest in complexation energy. For PM3 and PM7 suggest MBCD-I, on the other hand, PM6 is favorable MBCD-II. All inclusion complexes' geometries, which are performed by PCM calculation preserved the cone shape. However, the MD simulations reveal that MBCD complexes geometries are more distorted and fluctuated comparing to BCD and HPBCD. Due to, H-bond which are formed at the wider rim are broken from the methyl group. Hence, the MD simulation results suggest that HPBCD is the most suitable host for plumbagin encapsulation. The intermolecular hydrogen bond, van der Waals, and hydrophobic interactions play an important role in complexation process of plumbagin with BCDs.

For the release pathway of all the inclusion complexes, the MD simulations showed the released direction of guest molecule is from the wider side of the host

molecule. The favorable orientation of plumbagin molecule in BCD from MD results, the methyl quinone group of plumbagin was placed in the cavity of BCD, on the other hand, HPBCD inclusion complex, the methyl quinone group of plumbagin was point out to the wider rim.



REFERENCES

- Abdelmalek, L., Fatiha, M., Leila, N., Mouna, C., Nora, M., & Djameledine, K. (2016). Computational study of inclusion complex formation between carvacrol and β -cyclodextrin in vacuum and in water: Charge transfer, electronic transitions and NBO analysis. *Journal of Molecular Liquids*, 224, 62–71. <https://doi.org/10.1016/j.molliq.2016.09.053>
- Alvira, E. (2018). Theoretical study of the β -cyclodextrin inclusion complex formation of eugenol in water. *Molecules*, 23(4). <https://doi.org/10.3390/molecules23040928>
- Archimandritis, A. S., Papadimitriou, T., Kormas, K. A., Laspidou, C. S., Yannakopoulou, K., & Lazarou, Y. G. (2016). Theoretical investigation of microcystin-LR, microcystin-RR and nodularin-R complexation with α -, β -, and γ -cyclodextrin as a starting point for the targeted design of efficient cyanotoxin traps. *Sustainable Chemistry and Pharmacy*, 3, 25–32. <https://doi.org/10.1016/j.scp.2016.02.001>
- Aree, T., Arunchai, R., Koonrugsa, N., & Intasiri, A. (2012). Fluorometric and theoretical studies on inclusion complexes of β -cyclodextrin and d-, l-phenylalanine. *Spectrochimica Acta - Part A: Molecular and Biomolecular Spectroscopy*, 96, 736–743. <https://doi.org/10.1016/j.saa.2012.07.049>
- Aree, T., Hoier, H., Schulz, B., Reck, G., & Saenger, W. (2000). Novel Type of Thermostable Channel Clathrate Hydrate Formed by Heptakis(2,6-di-O-methyl)- β -cyclodextrin·15 H₂O—A Paradigm of the Hydrophobic Effect. *Angewandte Chemie International Edition*, 39(5), 897–899. [https://doi.org/10.1002/\(SICI\)1521-3773\(20000303\)39:5<897::AID-ANIE897>3.0.CO;2-R](https://doi.org/10.1002/(SICI)1521-3773(20000303)39:5<897::AID-ANIE897>3.0.CO;2-R)
- Astray, G., Gonzalez-Barreiro, C., Mejuto, J. C., Rial-Otero, R., & Simal-Gándara, J. (2009). A review on the use of cyclodextrins in foods. *Food Hydrocolloids*, 23(7), 1631–1640. <https://doi.org/10.1016/j.foodhyd.2009.01.001>
- Bani-Yaseen, A. D. (2016). Computational Molecular Perspectives on the Interaction of Propranolol with β -Cyclodextrin in Solution: Towards the Drug-Receptor Mechanism of Interaction. *Journal of Molecular Liquids*. <https://doi.org>

/10.1016/j.molliq.2016.12.023

- Bouhadiba, A., Belhocine, Y., Rahim, M., Djilani, I., Nouar, L., & Khatmi, D. E. (2017). Host-guest interaction between tyrosine and β -cyclodextrin: Molecular modeling and nuclear studies. *Journal of Molecular Liquids*, 233, 358–363. <https://doi.org/10.1016/j.molliq.2017.03.029>
- Bouzitouna, A., Khatmi, D., & Attoui-Yahia, O. (2016). A hybrid MP2/DFT scheme for N-Nitroso-N-(2-chloroethyl)-N'-sulfamoylproline/ β -Cyclodextrin supra-molecular structure: AIM, NBO analysis. *Computational and Theoretical Chemistry*. <https://doi.org/10.1016/j.comptc.2016.12.004>
- Burodom, A., & Itharat, A. (2013). Inflammatory suppressive effect of Benjakul , a Thai traditional medicine on intestinal epithelial cell line. *Journal of Medicinal Plants Research*, 7(44), 3286–3291. <https://doi.org/https://doi.org/10.5897/JMPR2013.5206>
- Carvalho, L. B. de, Burusco, K. K., Jaime, C., Venâncio, T., Carvalho, A. F. S. de, Murgas, L. D. S., & Pinto, L. de M. A. (2018). Complexes between methyltestosterone and β -cyclodextrin for application in aquaculture production. *Carbohydrate Polymers*, 179(June 2017), 386–393. <https://doi.org/10.1016/j.carbpol.2017.09.023>
- Case, D. A. (2018). Amber 18. *University of California, San Francisco*.
- Connors, K. A. (1997). The Stability of Cyclodextrin Complexes in Solution. *Chemical Reviews*, 97(5), 1325–1358. <https://doi.org/10.1021/cr960371r>
- Dandawate, P., Vemuri, K., Venkateswara Swamy, K., Khan, E. M., Sritharan, M., & Padhye, S. (2014). Synthesis, characterization, molecular docking and anti-tubercular activity of Plumbagin-Isoniazid Analog and its β -cyclodextrin conjugate. *Bioorganic and Medicinal Chemistry Letters*, 24(21), 5070–5075. <https://doi.org/10.1016/j.bmcl.2014.09.032>
- Dass, C. R., & Jessup, W. (2000). Apolipoprotein A-I, cyclodextrins and liposomes as potential drugs for the reversal of atherosclerosis. A review. *The Journal of Pharmacy and Pharmacology*, 52(7), 731–761. <https://doi.org/10.1211/0022357001774606>
- De Paiva, S. R., Figueiredo, M. R., Aragão, T. V., & Coelho Kaplan, M. A. (2003). Antimicrobial Activity in Vitro of Plumbagin Isolated from Plumbago Species.

- Memorias Do Instituto Oswaldo Cruz*, 98(7), 959–961. <https://doi.org/10.1590/S0074-02762003000700017>
- de Sousa Araújo, T. A., de Melo, J. G., Júnior, W. S. F., & Albuquerque, U. P. (2016). Medicinal Plants. In *Introduction to Ethnobiology* (pp. 143–149). https://doi.org/10.1007/978-3-319-28155-1_22
- Del Valle, E. M. M. (2004). Cyclodextrins and their uses: A review. *Process Biochemistry*, 39(9), 1033–1046. [https://doi.org/10.1016/S0032-9592\(03\)00258-9](https://doi.org/10.1016/S0032-9592(03)00258-9)
- Djilani, I., Nouar, L., Madi, F., Haiahem, S., Bouhadiba, A., & Khatmi, D. (2014). Molecular modeling study of neutral and cationic species of ortho-anisidine by β -cyclodextrin. In *Advances in Quantum Chemistry* (Vol. 68). <https://doi.org/10.1016/B978-0-12-800536-1.00015-0>
- Eid, E. E. M., Abdul, A. B., Suliman, F. E. O., Sukari, M. A., Rasedee, A., & Fatah, S. S. (2011). Characterization of the inclusion complex of zerumbone with hydroxypropyl- β -cyclodextrin. *Carbohydrate Polymers*, 83(4), 1707–1714. <https://doi.org/10.1016/j.carbpol.2010.10.033>
- Grimme, S. (2011). Density functional theory with London dispersion corrections. *Wiley Interdisciplinary Reviews: Computational Molecular Science*, 1(2), 211–228. <https://doi.org/10.1002/wcms.30>
- Grimme, S., Antony, J., Ehrlich, S., & Krieg, H. (2010). A consistent and accurate ab initio parametrization of density functional dispersion correction (DFT-D) for the 94 elements H-Pu. *Journal of Chemical Physics*, 132(15). <https://doi.org/10.1063/1.3382344>
- Hanpaibool, C., Chakcharoensap, T., Arifin, Hijikata, Y., Irle, S., Wolschann, P., ... Rungrotmongkol, T. (2018). Theoretical analysis of orientations and tautomerization of genistein in β -cyclodextrin. *Journal of Molecular Liquids*, 265, 16–23. <https://doi.org/10.1016/j.molliq.2018.05.109>
- Harata, K., Rao, C. T., Pitha, J., Fukunaga, K., & Uekama, K. (1991). Crystal structure of 2-O-[(S)-2-hydroxypropyl]cyclomaltoheptaose. *Carbohydrate Research*, 222, 37–45. Retrieved from <http://www.ncbi.nlm.nih.gov/pubmed/1813110>
- Hehre, W. J. (2003). *A Guide to Molecular Mechanics and Quantum Chemical Calculations*. Retrieved from <https://www.wavefun.com/support/AGuidetoMM.pdf>

- Hsu, Y.-L. (2006). Plumbagin (5-Hydroxy-2-methyl-1,4-naphthoquinone) Induces Apoptosis and Cell Cycle Arrest in A549 Cells through p53 Accumulation via c-Jun NH2-Terminal Kinase-Mediated Phosphorylation at Serine 15 in Vitro and in Vivo. *Journal of Pharmacology and Experimental Therapeutics*, 318(2), 484–494. <https://doi.org/10.1124/jpet.105.098863>
- Lawtrakul, L., Inthajak, K., & Toochinda, P. (2014). Molecular calculations on β -cyclodextrin inclusion complexes with five essential oil compounds from *Ocimum basilicum* (sweet basil). *ScienceAsia*, 40(2), 145–151. <https://doi.org/10.2306/scienceasia1513-1874.2014.40.145>
- Leila, N., Sakina, H., Bouhadiba, A., Fatiha, M., & Leila, L. (2011). Molecular modeling investigation of para-nitrobenzoic acid interaction in β -cyclodextrin. *Journal of Molecular Liquids*, 160(1), 1–7. <https://doi.org/10.1016/j.molliq.2011.02.004>
- Li, X.-S., Liu, L., Mu, T.-W., & Guo, Q.-X. (2000a). A Systematic Quantum Chemistry Study on Cyclodextrins. *Monatshefte Für Chemie*, 131, 849–855. Retrieved from <http://download.springer.com/static/pdf/215/art%253A10.1007%252Fs007060070062.pdf?originUrl=http%3A%2F%2Flink.springer.com%2Farticle%2F10.1007%2Fs007060070062&token2=exp=1497861805~acl=%2Fstatic%2Fpdf%2F215%2Fart%25253A10.1007%25252Fs007060070062.pdf%3For>
- Li, X.-S., Liu, L., Mu, T.-W., & Guo, Q.-X. (2000b). A Systematic Quantum Chemistry Study on Cyclodextrins. *Monatshefte Für Chemie/Chemical Monthly*, 131(8), 849–855. <https://doi.org/10.1007/s007060070062>
- Lichtenthaler, F. W., & Immel, S. (1996). Towards Understanding Formation and Stability of Cyclodextrin Inclusion Complexes: Computation and Visualization of their Molecular Lipophilicity Patterns[1]. *Starch - Starke*, 48(4), 145–154. <https://doi.org/10.1002/star.19960480405>
- LOFTSSON, T., & DUCHENE, D. (2007). Cyclodextrins and their pharmaceutical applications. *International Journal of Pharmaceutics*, 329(1–2), 1–11. <https://doi.org/10.1016/j.ijpharm.2006.10.044>
- M. J. Frisch and G. W. Trucks and H. B. Schlegel and G. E. Scuseria and M. A. Robb and J. R. Cheeseman and G. Scalmani and V. Barone and G. A. Petersson and H. Nakatsuji and X. Li and M. Caricato and A. V. Marenich and J. Bloino and B. G.

- Janesko and R. G, J. A. and J. E. P. and F. O. and M. J. B. and J. J. H. and E. N. B. and K. N. K. and V. N. S. and T. A. K. and R. K. and J. N. and K. R. and A. P. R. and J. C. B. and S. S. I. and J. (2016). *Gaussian 16*.
- Magnusdottir, A., Másson, M., & Loftsson, T. (2002). Self association and cyclodextrin solubilization of NSAIDs. *Journal of Inclusion Phenomena*, 44(1–4), 213–218. <https://doi.org/10.1023/A:1023079322024>
- Martínez-Alonso, A., Losada-Barreiro, S., & Bravo-Díaz, C. (2015). Encapsulation and solubilization of the antioxidants gallic acid and ethyl, propyl and butyl gallate with β -cyclodextrin. *Journal of Molecular Liquids*, 210, 143–150. <https://doi.org/10.1016/j.molliq.2014.12.016>
- Messiad, H., Yousfi, T., Djemil, R., & Amira-Guebailia, H. (2016). Modeling of the inclusive complexation of natural drug trans 3,5,3',4'-tetrahydroxystilbene with β -cyclodextrin. *Comptes Rendus Chimie*, 1–10. <https://doi.org/10.1016/j.crci.2016.08.008>
- Milla, R. D. and T. K. and J. (2009). *GaussView 5.0*.
- Minoru Sakurai, Masaki Kitagawa, Hajime Hoshi, Yoshio Inoue, R. C. (1990). A molecular orbital study of cyclodextrin (cyclomalto- oligosaccharide) inclusion complexes. Iii, dipole moments of cyclodextrins in various types of inclusion complex. *Carbohydrate Research*, 198, 181–191.
- Morris, G. M., Huey, R., Lindstrom, W., Sanner, M. F., Belew, R. K., Goodsell, D. S. and Olson, A. J. (2009). *AutoDock4 and AutoDockTools4*. University of California, San Francisco.
- Morris, G. M., Goodsell, D. S., Halliday, R. S., Huey, R., Hart, W. E., Belew, R. K., & Olson, A. J. (1998). Automated docking using a Lamarckian genetic algorithm and an empirical binding free energy function. *Journal of Computational Chemistry*, 19(14), 1639–1662. [https://doi.org/10.1002/\(SICI\)1096-987X\(19981115\)19:14<1639::AID-JCC10>3.0.CO;2-B](https://doi.org/10.1002/(SICI)1096-987X(19981115)19:14<1639::AID-JCC10>3.0.CO;2-B)
- Nutho, B., Nunthaboot, N., Wolschann, P., Kungwan, N., & Rungrotmongkol, T. (2017). Metadynamics supports molecular dynamics simulation-based binding affinities of eucalyptol and beta-cyclodextrin inclusion complexes. *RSC Advances*, 7(80), 50899–50911. <https://doi.org/10.1039/c7ra09387j>
- Oommen, E., Shenoy, B. D., Udupa, N., Kamath, R., & Devi, P. U. (1999). Antitumour

- Efficacy of Cyclodextrin-complexed and Niosome- encapsulated Plumbagin in Mice Bearing Melanoma B16F1. *Pharmacy and Pharmacology Communications*, 5(4), 281–285. <https://doi.org/10.1211/146080899128734857>
- Pawar, A., Patel, R., Arulmozhi, S., & Bothiraja, C. (2016). D- α -Tocopheryl polyethylene glycol 1000 succinate conjugated folic acid nanomicelles: Towards enhanced bioavailability, stability, safety, prolonged drug release and synergized anticancer effect of plumbagin. *RSC Advances*, 6(81), 78106–78121. <https://doi.org/10.1039/c6ra12714b>
- Pettersen, E. F., Goddard, T. D., Huang, C. C., Couch, G. S., Greenblatt, D. M., Meng, E. C., & Ferrin, T. E. (2004). UCSF Chimera - A visualization system for exploratory research and analysis. *Journal of Computational Chemistry*, 25(13), 1605–1612. <https://doi.org/10.1002/jcc.20084>
- Qi, Z. H., & Hedges, A. R. (1997). *Use of Cyclodextrins for Flavors*. <https://doi.org/10.1021/bk-1995-0610.ch018>
- Qingzhong, L., Wang, N., & Zhiwu, Y. (2007). Effect of hydration on the C–H \cdots O hydrogen bond: A theoretical study. *Journal of Molecular Structure: THEOCHEM*, 847(1–3), 68–74. <https://doi.org/10.1016/j.theochem.2007.08.035>
- R.D'Souza, U.V.Singh, K.S.Aithal, & M.Udupa. (1997). *Antifertility Activity of Niosomal HPbCD-Plumbagin complex*. 36–40.
- Rahim, M., Madi, F., Nouar, L., Bouhadiba, A., Haiahem, S., Khatmi, D. E., & Belhocine, Y. (2014). Driving forces and electronic structure in β -cyclodextrin/3,3'-diaminodiphenylsulphone complex. *Journal of Molecular Liquids*, 199, 501–510. <https://doi.org/10.1016/j.molliq.2014.09.035>
- Rajewski, R. A., & Stella, V. J. (1996). Pharmaceutical applications of cyclodextrins. 2. In vivo drug delivery. *Journal of Pharmaceutical Sciences*, 85(11), 1142–1169. <https://doi.org/10.1021/js960075u>
- Rasheed, A., Kumar C.K., A., & Sravanthi, V. V. N. S. S. (2008). Cyclodextrins as drug carrier molecule: A review. *Scientia Pharmaceutica*, 76(4), 567–598. <https://doi.org/10.3797/scipharm.0808-05>
- Rasmussen, K., Vlasenko, K., Svanholt, H., Almenningen, A., Bastiansen, O., Braathen, G., ... Cyvin, S. J. (1982). Conformation and Anomer Ratio of D-Glucopyranose in Different Potential Energy Functions. *Acta Chemica*

- Scandinavica*, 36a, 323–327. <https://doi.org/10.3891/acta.chem.scand.36a-0323>
- Rattarom, R., Sakpakdeejaroen, I., & Itharat, A. (2010). *Cytotoxic effects of the ethanolic extract from Benjakul formula and its compounds on human lung cancer cells*. 32(1), 99–101.
- Risch, S. J. (1995). *Encapsulation: Overview of Uses and Techniques*. <https://doi.org/10.1021/bk-1995-0590.ch001>
- Rischer, H., Hamm, A., & Bringmann, G. (2002). Nepenthes insignis uses a C2-portion of the carbon skeleton of l-alanine acquired via its carnivorous organs, to build up the allelochemical plumbagin. *Phytochemistry*, 59(6), 603–609. [https://doi.org/10.1016/S0031-9422\(02\)00003-1](https://doi.org/10.1016/S0031-9422(02)00003-1)
- Saenger, W., & Steiner, T. (1998). Cyclodextrin Inclusion Complexes: Host-Guest Interactions and Hydrogen-Bonding Networks. *Acta Crystallographica Section A: Foundations of Crystallography*, 54(6), 798–805. <https://doi.org/10.1107/S0108767398010733>
- Saetung, A., Itharat, A., Dechsukum, C., Wattanapiromsakul, C., & Keaw, Niwat Keawpradub, and P. R. (2005). Cytotoxic activity of Thai medicinal plants for cancer treatment. *J Sci Technol*, 27(Suppl. 2), 469–478. <https://doi.org/10.1055/s-0028-1084234>
- Sancho, M. I., Gasull, E., Blanco, S. E., & Castro, E. A. (2011). Inclusion complex of 2-chlorobenzophenone with cyclomaltoheptaose (β -cyclodextrin): Temperature, solvent effects and molecular modeling. *Carbohydrate Research*, 346(13), 1978–1984. <https://doi.org/10.1016/j.carres.2011.05.002>
- Sangpheak, W., Kicuntod, J., Schuster, R., Rungrotmongkol, T., Wolschann, P., Kungwan, N., ... Pongsawasdi, P. (2015). Physical properties and biological activities of hesperetin and naringenin in complex with methylated β -cyclodextrin. *Beilstein Journal of Organic Chemistry*, 11, 2763–2773. <https://doi.org/10.3762/bjoc.11.297>
- Seridi, S., Seridi, A., Berredjem, M., & Kadri, M. (2013). Host-guest interaction between 3,4-dihydroisoquinoline-2(1H)-sulfonamide and β -cyclodextrin: Spectroscopic and molecular modeling studies. *Journal of Molecular Structure*, 1052, 8–16. <https://doi.org/10.1016/j.molstruc.2013.08.035>
- Shaikh, J., Pradhan, R., Dandawate, P., Subramaniam, D., Ponnurangam, S., Martis, E.

- F., ... Anant, S. (2017). Spectral and Molecular Modeling Studies on the Influence of β -Cyclodextrin and Its Derivatives on Albendazole and Its Anti-Proliferative Activity Against Pancreatic Cancer Cells. *Journal of Pharmaceutical Sciences and Pharmacology*, 3(1), 1–14. <https://doi.org/10.1166/jpsp.2017.1075>
- Singh, M., Sharma, R., & Banerjee, U. C. (2002). Biotechnological applications of cyclodextrins. *Biotechnology Advances*, 20(5–6), 341–359. Retrieved from <http://www.ncbi.nlm.nih.gov/pubmed/14550020>
- Singh, U. V., & Udupa, N. (1997). Reduced toxicity and enhanced antitumor efficacy of betacyclodextrin plumbagin inclusion complex in mice bearing Ehrlich ascites carcinoma. *Indian Journal of Physiology and Pharmacology*, 41(2), 171–175.
- Sompornpisut, P., Deechalao, N., & Vongsvivut, J. (2002). An Inclusion Complex of beta-Cyclodextrin-LPhenylalanine: ¹H NMR and Molecular Docking Studies. *ScienceAsia*, 28(3), 263. <https://doi.org/10.2306/scienceasia1513-1874.2002.28.263>
- Son, T. G., Camandola, S., Arumugam, T. V., Cutler, R. G., Telljohann, R. S., Mughal, M. R., ... Mattson, M. P. (2010). Plumbagin, a novel Nrf2/ARE activator, protects against cerebral ischemia. *Journal of Neurochemistry*, 112(5), 1316–1326. <https://doi.org/10.1111/j.1471-4159.2009.06552.x>
- Srihakulung, O., Lawtrakul, L., Toochinda, P., Kongprawechnon, W., Intarapanich, A., & Maezono, R. (2018). Theoretical investigation of molecular calculations on inclusion complexes of plumbagin with β -cyclodextrins. *Proceedings of the 4th Asian Conference on Defence Technology, ACDT 2017, 2018-Janua*. <https://doi.org/10.1109/ACDTJ.2017.8259589>
- Srihakulung, Ornin. (2018). *Molecular Interactions in Inclusion of Complexes with Cyclodextrins* (Japan Advanced Institute of Science and Technology). Retrieved from <http://hdl.handle.net/10119/15527>
- Srihakulung, Ornin, Lawtrakul, L., Toochinda, P., Kongprawechnon, W., Intarapanich, A., & Maezono, R. (2017). Theoretical investigation of molecular calculations on inclusion complexes of plumbagin with β -cyclodextrins. *2017 Fourth Asian Conference on Defence Technology - Japan (ACDT)*, 1–5. <https://doi.org/10.1109/ACDTJ.2017.8259589>
- Steiner, T., & Koellner, G. (1994). Crystalline β -Cyclodextrin Hydrate at Various

- Humidities: Fast, Continuous, and Reversible Dehydration Studied by X-ray Diffraction. *Journal of the American Chemical Society*, 116(12), 5122–5128. <https://doi.org/10.1021/ja00091a014>
- Stewart, J. J.P., Császár, P., & Pulay, P. (1982). Fast semiempirical calculations. *Journal of Computational Chemistry*, 3(2), 227–228. <https://doi.org/10.1002/jcc.540030214>
- Stewart, James J. P. (2007). Optimization of parameters for semiempirical methods V: Modification of NDDO approximations and application to 70 elements. *Journal of Molecular Modeling*, 13(12), 1173–1213. <https://doi.org/10.1007/s00894-007-0233-4>
- Stewart, James J.P. (2013). Optimization of parameters for semiempirical methods VI: More modifications to the NDDO approximations and re-optimization of parameters. *Journal of Molecular Modeling*, 19(1), 1–32. <https://doi.org/10.1007/s00894-012-1667-x>
- Sugie, S., Okamoto, K., Rahman, K. M., Tanaka, T., Kawai, K., Yamahara, J., & Mori, H. (1998). Inhibitory effects of plumbagin and juglone on azoxymethane-induced intestinal carcinogenesis in rats. *Cancer Letters*, 127(1–2), 177–183. Retrieved from <http://www.ncbi.nlm.nih.gov/pubmed/9619875>
- Suliman, F. O., & Elbashir, A. A. (2012). Enantiodifferentiation of chiral baclofen by β -cyclodextrin using capillary electrophoresis: A molecular modeling approach. *Journal of Molecular Structure*, 1019, 43–49. <https://doi.org/10.1016/j.molstruc.2012.03.055>
- Suthanurak, M., Sakpakdeejaroen, I., Rattarom, R., & Itharat, A. (2010). Formulation and stability test of BJ adaptogen tablets for cancer treatment. *Planta Medica*, 76(12), 160–163. Retrieved from <http://www.embase.com/search/results?subaction=viewrecord&from=export&id=L70447518><http://dx.doi.org/10.1055/s-0030-1264400><http://sfx.umd.edu/hs?sid=EMBASE&issn=00320943&id=doi:10.1055/s-0030-1264400&atitle=Formulation+and+stability+test+of+BJ+adaptogen+>
- Szejtli, J. (1998). Introduction and General Overview of Cyclodextrin Chemistry. *Chemical Reviews*, 98(5), 1743–1754. <https://doi.org/10.1021/cr970022c>
- Tinoco, I., & Wen, J. Der. (2009). Simulation and analysis of single-ribosome

- translation. *Physical Biology*, 6(2). <https://doi.org/10.1088/1478-3975/6/2/025006>
- Tomasi, J., Mennucci, B., & Cammi, R. (2005). Quantum Mechanical Continuum Solvation Models. *Chemical Reviews*, 105(8), 2999–3094. <https://doi.org/10.1021/cr9904009>
- van der Vijver, L. M. (1972). Distribution of plumbagin in the mplantumbaginaceae. *Phytochemistry*, 11(11), 3247–3248. [https://doi.org/10.1016/S0031-9422\(00\)86380-3](https://doi.org/10.1016/S0031-9422(00)86380-3)
- Villiers, A. C. (1891). Sur la transformation de la fécule en dextrine par le ferment butyrique. *Seances Acad. Sci.*, 112(536–538).
- Voityuk, A. A., & Rösch, N. (2000). AM1/d Parameters for Molybdenum. *Journal of Physical Chemistry A*, 104(17), 4089–4094. <https://doi.org/10.1021/jp994394w>
- Xia, Y., Wang, X., Zhang, Y., & Luo, B. (2011). Theoretical Study on Interactions of β -cyclodextrin with Trans-dichloro(dipyridine) platinum(II). *Computational and Theoretical Chemistry*, 967(2–3), 213–218. <https://doi.org/10.1016/j.comptc.2011.03.010>
- Xu, F., Yang, Q., Wu, L., Qi, R., Wu, Y., Li, Y., ... Liu, B. (2017). Investigation of inclusion complex of patchouli alcohol with β -cyclodextrin. *PLoS ONE*, 12(1), 1–10. <https://doi.org/10.1371/journal.pone.0169578>
- Zhang, M. K., Lyu, Y., Zhu, X., Wang, J. P., Jin, Z. Y., & Narsimhan, G. (2018). Enhanced solubility and antimicrobial activity of alamethicin in aqueous solution by complexation with γ -cyclodextrin. *Journal of Functional Foods*, 40(August 2017), 700–706. <https://doi.org/10.1016/j.jff.2017.12.021>
- Zhao, Y., Schultz, N. E., & Truhlar, D. G. (2006). Design of density functionals by combining the method of constraint satisfaction with parametrization for thermochemistry, thermochemical kinetics, and noncovalent interactions. *Journal of Chemical Theory and Computation*, 2(2), 364–382. <https://doi.org/10.1021/ct0502763>

APPENDICES



APPENDIX A

SEMI-EMPIRICAL METHODS

There are many ways to consider the electron-electron interactions when the molecules overlap. Normally, we can separate the interactions in three groups.

1. The extended Hückel method

This method neglects all electron-electron interactions that can make the computation very fast but not accurate.

2. Neglect of differential overlap (NDO) model

This method can neglect some of electron-electron interactions. The Hartree-Fock Self-Consistent Field (HF-SCF) is used to solve the Schrödinger equation with various approximations. The model includes; CNDO, INDO, MINDO/3, ZINDO/1 and ZINDO/S.

3. Neglect of Diatomic Differential Overlap (NDDO)

This model is a modern semi-empirical model which is based on INDO and included the overlap density between two orbitals on one atom interacting with the same or another atom.

- a) Parameterized Model number 3 (PM3)

This calculation utilizes the semi-empirical method for the quantum calculation of electronic structure. This method employs modern semi-empirical model or NDDO, and it is accurate to some degree (Pettersen et al., 2004). On the other hand, previous work (Aree, Arunchai, Koonrugs, & Intasiri, 2012; Li, Liu, Mu, & Guo, 2000a) compared the accuracy for gas phase heats of formation (HOF), the results of accuracy have been shown in the increasing in the order of PM3 < PDDG < PM6. DDO is ignored in integral approximation is used for the calculation. Elements that have been parametrized in PM3 include H, C, N, O, F, Al, Si, P, S, Cl, Br, I, Ca, Ti, V, Cr, Mn, Fe, Co, Ni, Cu, Zn, Zr, Mo, Tc, Ru, Rh, Pd, Hf, Ta, W, Re, Os, Ir, Pt, and Gd. Various number metals have been parameterized in later work. The cyclodextrins inclusion complex studies get the coincide binding energy result with the experimental observations from PM3. PM3 deals with hydrogen bond (O-H...O) and reproduces the

crystalline structure relatively well (Hehre, 2003; Li, Liu, Mu, & Guo, 2000b). As a result, PM3 was selected for the calculation in several studies (Aree et al., 2012) including our previous work (Srihakulung et al., 2018). PM6 method (James & Stewart, 2007) adds some improvement of PM3 in the geometries prediction, for instance, replacing Gaussian core-core corrections to core-core correction introduced by Voityuk & Rösch, 2000.

b) Parameterized Model number 6 (PM6)

PM6 performs pairwise parameter and also uses different core-core repulsion potentials for N-H, O-H, C-C and Si-O which also improve some weaknesses in the parametrization. The previous studies also show good performance of this method in cyclodextrin inclusion complex system, which improves the stability of inclusion complex structure by adding damping functional (Rahim et al., 2014; Xia, Wang, Zhang, & Luo, 2011). Some works (Suliman & Elbashir, 2012) express the thermodynamic parameters results from PM6 in gas and water according to MD simulations and the experiment as results (Eid et al., 2011; Sancho, Gasull, Blanco, & Castro, 2011; Seridi et al., 2013).

c) Parameterized Model number 7 (PM7)

PM7 method (James & Stewart, 2013) improves some part of PM6 appending explicit terms to describe non-covalent interactions or non-bonding interaction, for instance, hydrophobic-hydrophobic interactions and long range bonding interaction or hydrogen bond, which is the interaction between host-guest of our system. The accuracy of this method can be compared to the higher level of theoretical methods, while requiring of low computational cost. This method also provides good results in ΔG° , ΔH° and ΔS comparing to the experimental value (Yaseen, 2016). Basically, PM7 illustrates high value of $\Delta E_{\text{HOMO-LUMO}}$ energy gap of BCD molecule with CENs-prolinate, which means that the compound is stable (Bouzitouna, Khatmi, & Attoui-Yahia, 2016). PM7 is also successful used to predict the parameter of geometry structure and reactive trend in complex between microcystins and nodularins with cyclodextrin (Archimandritis et al., 2016). On the other hand, there are some limitations of this method including large error for the non-covalent interaction energy (Eid et al., 2011)

APPENDIX B

POLARIZABLE CONTINUUM MODEL

The Polarizable Continuum Model (PCM) was reported by Tomasi, Mennucci, & Cammi, 2005 is one of the most frequently used continuum solvation methods and has seen numerous variations over the years. The PCM model calculates the molecular free energy in solution as the sum over three terms:

$$G_{sol} = G_{es} + G_{dr} + G_{cav} \quad (B.1)$$

These components represent the electrostatic (es) and the dispersion-repulsion (dr) contributions to the free energy, and the cavitation energy (cav). All three terms are calculated using a cavity defined through interlocking van der Waals-spheres centered at atomic positions. The reaction field is represented through point charges located on the surface of the molecular cavity (Apparent Surface Charge (ASC) model). The particular version of PCM that will be discussed here is the one using the United Atom for Hartree-Fock (UAHF) model to build the cavity. In this model the vdW-surface is constructed from spheres located on heavy (that is, non-hydrogen) elements only (United Atom approach). The vdW-radius of each atom is a function of atom type, connectivity, overall charge of the molecule, and the number of attached hydrogen atoms. In evaluating the three terms in equation 3.4 this cavity is used in slightly different ways. While calculation of the cavitation energy G_{cav} uses the surface defined by the van der Waals spheres, the solvent accessible surface is used to calculate the dispersion-repulsion contribution G_{dr} to the solution free energy. The latter differs from the former through additional consideration of the (idealized) solvent radius. The electrostatic contribution to the free energy in solution G_{es} uses an approximate version of the solvent excluding surface constructed through scaling all radii by a constant factor (e.g. 1.2 for water) and then adding some more spheres not centered on atoms in order to arrive at a somewhat smoother surface.

The keyword for Gaussian 16 program for PCM calculation (SCRF=PCM, DPCM, CPCM or IEFPCM) may be specified in an additional blank-line terminated

input section provided that the Read option is also specified. Keywords within this section follow general Gaussian input rules. The available keywords are listed at the end of the manual section for the SCRF keyword.

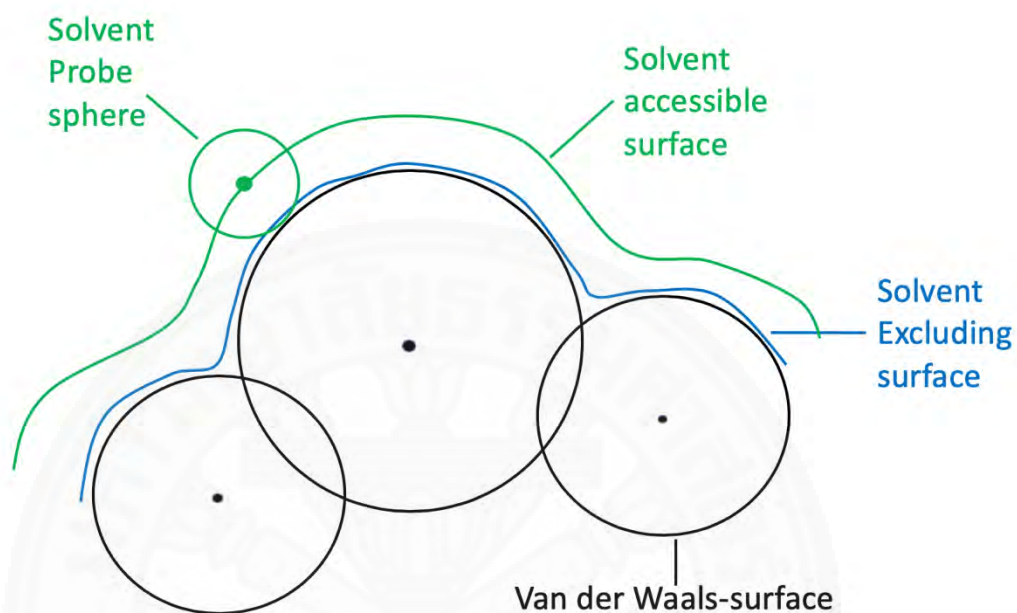


Figure B.1 Schematic picture of van der Waals surface

APPENDIX C

MOLECULAR DOCKING SIMULATION

AutoDock is one tool, which predict how match between ligand and the host which is the biomacromolecular molecule from the interaction between them. Normally this program is used in computer-aided drug design to find the candidate molecule with their targets. Search and score method are used for finding the configuration space available for interaction between ligand and host. Evaluation the occurrence, the scoring system is used to find the binding energy. AutoDock 4.2.6 use the Lamarckian Genetic Algorithm and empirical free energy to score the result. Scoring function makes the calculation faster, that can be used for the larger systems. A semi-empirical free energy force field is used for evaluating the conformation during the docking simulation. The force fields were parameterized by the large number of protein and inhibitor complexes into inhibition constants or K_i . The force field includes six pairwise evaluations (V) and the conformational entropy lost during the formation (ΔS_{conf}), where L means ligand, P mean Protein and P-L is the conformation between ligand and protein.

$$\Delta G = (V_{bound}^{L-L} - V_{unbound}^{L-L}) + (V_{bound}^{P-P} - V_{unbound}^{P-P}) + (V_{bound}^{P-L} - V_{unbound}^{P-L} + \Delta S_{conf}) \quad (C.1)$$

For each of pair-wise energetic terms evaluate all of the energy from dispersion-repulsion, hydrogen bonding, desolvation and electrostatics as the following equation. W is the weight constant, which is evaluated from the optimization of semi-empirical free energy based on the binding constant from the experimental data.

$$V = W_{vdw} \sum_{i,j} \left(\frac{A_{ij}}{r_{ij}^{12}} - \frac{B_{ij}}{r_{ij}^6} \right) + W_{h-bond} \sum_{i,j} E(t) \left(\frac{C_{ij}}{r_{ij}^{12}} - \frac{D_{ij}}{r_{ij}^6} \right) + W_{elect} \sum_{i,j} \left(\frac{q_i q_j}{e(r_{ij}) r_{ij}} \right) + W_{sol} \sum_{i,j} (S_i V_j + S_j V_i) e^{(-r_{ij}^2 / 2\sigma^2)} \quad (C.2)$$

The first term is dispersion and repulsion interactions (6 / 12 potential for dispersion/repulsion interaction), which the parameter based on Amber force field. The

second term is hydrogen bond term; C and D are the maximal of bonding, hydrogen bond with oxygen and nitrogen is 5 kcal/mol (1.9 Å) for hydrogen bond with sulfur is 1 kcal/mol (2.5 Å). The function $E(t)$ base on the angle t , which in the ideal position of hydrogen. The third term is the screen Coulomb potential for electrostatics. For the forth term, the desolvation potential, which base on volume (V) and solvation parameter (S) and exponential term is distance weighing factor $\sigma = 3.5$ Å.

The genetic algorithm (GA) is used to describe in orientation, translation and conformation of ligand and protein arrangement (Morris et al., 1998). The algorithm begins after created the random population of individuals, which are set by the user. The orientations are given a random in unit vector and rotation angle between -180 and +180 degree. In addition, there is a number generator, which is the independent hardware. It produces the random initial population follow by loop over generations and repeat until reach the maximum number of evaluation. The most recent generator, which AutoDock 4.2.6 used, is LGA or Lamarckian Genetic Algorithm. This algorithm uses Darwinian evolution as the major characteristics and apply the Mendelian genetics.

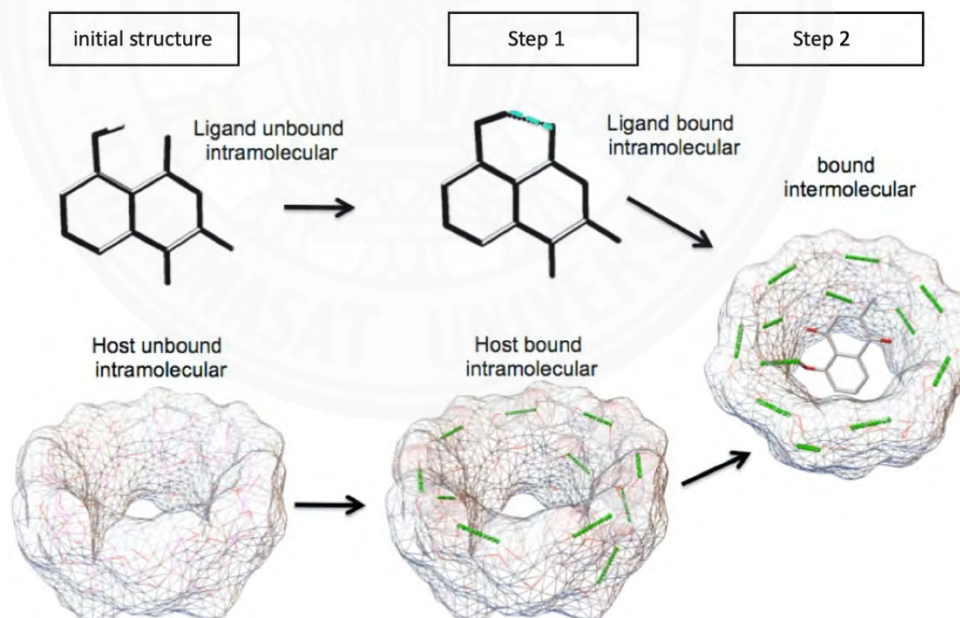


Figure C.1 Scoring function based on the AMBER force field is evaluated binding of the molecules in two steps, the first is intramolecular force in monomer molecule and then the intermolecular force between ligand and host are evaluated.

APPENDIX D

MOLECULAR DYNAMICS SIMULATION

Molecular dynamics simulation is normally used to investigate the structure, dynamics and thermodynamics of biological molecules and their complexes, which describe properties, pattern and strength of many biological systems behavior, such as drug receptor interaction, membrane embedded protein and large macromolecular complexes like ribosomes system (Tinoco & Wen, 2009). This method calculates the time dependent behavior of a molecular system. In the most common version, the trajectories of atoms and molecules are determined by numerically solving Newton's equations of motion for a system of interacting particles, where forces between the particles and their potential energies are often calculated using interatomic potentials or molecular mechanics force fields. Normally almost types of medicine are developed to use under human body, which are full of water. Therefore, our research needs to consider under the solution effect to make our prediction more precise to the realistic condition. There are mainly two models to consider solvation systems, explicit and implicit models as was shown in figure D.1.

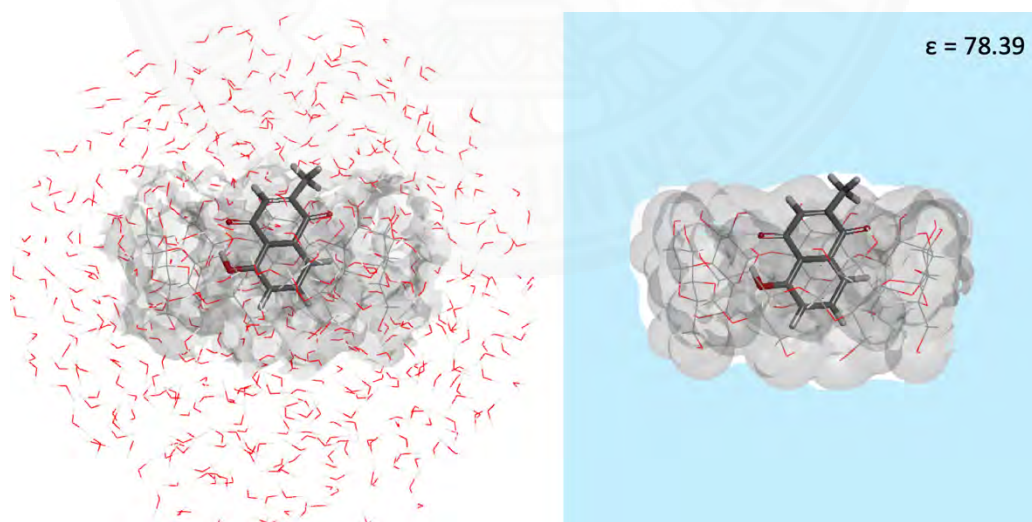


Figure D.1 Two types of solvation model, which included (left) explicit and (right) implicit solvation

- Explicit Solvent models: the region of interest is solvated in water sphere at 1 atm. The water molecules are submitted to an additional force field that restrain them in the sphere while maintaining a strong semblance to bulk water.

Includes individual solvent molecules.

Calculate the free energy by simulating solute-solvent interactions.

For example; Monte Carlo (MC) and molecular dynamics (MD) simulations.

Time consuming calculation.

Requires an empirical interaction potential between the solvent and solute, and between the solvent molecules.

The fully solvated central cell is simulated, in the environment produced by the repetition of this cell in all directions.

- Implicit Solvent Model

Solvent is treated as a polarizable continuum with a dielectric constant, ϵ , instead of explicit solvent molecules.

The charge distribution of the solute polarizes the solvent producing a reaction potential.

The reaction potential of solvent alters the solute. Interactions must be computed self consistently. Significantly cheaper than explicit solvent models.

Cannot model specific interactions such as hydrogen bonds.

For this research we consider both types of solvent models. The implicit model which is interested is Polarizable Continuum Model or PCM. In this research we consider this model for the first step. Then the explicit model as MD calculation was performed.

Glycam force field is used for carbohydrate systems. The latest version is GLYCAM06, which is more dependency on AMBER force field comparing to the previous version or GLYCAM04. The new GLYCAM is no longer limited to any particular classes of biomolecules but is extendible to all molecular classes in the spirit of a small-molecule force field. The torsion terms in the present work were all derived

from quantum mechanical data from a collection of minimal molecular fragments and related small molecules. For carbohydrates, there is now a single parameter set applicable to both α - and β -anomers and to all monosaccharide ring sizes and conformations. We demonstrate that deriving dihedral parameters by fitting to QM data for internal rotational energy curves for representative small molecules generally leads to correct rotamer populations in molecular dynamics simulations, and that this approach removes the need for phase corrections in the dihedral terms.

Parameterization of GLYCAM06 employed training and test sets of almost 100 molecules from the chemical families of hydrocarbons, alcohols, ethers, amides, esters, carboxylates, molecules of mixed functional groups as well as simple ring systems related to cyclic carbohydrates

The GLYCAM06 parameter set has begun to expand beyond the set of residues treated by the three-letter naming convention for residues. Here, we introduce three alternate classes of residue codes: four-letter codes, three-letter codes with non-standard naming, and codes where the anomeric configuration is specified by case in the third character.

In general, to understand any particular code, it is necessary to consult documentation associated with the release of the residue structural data.

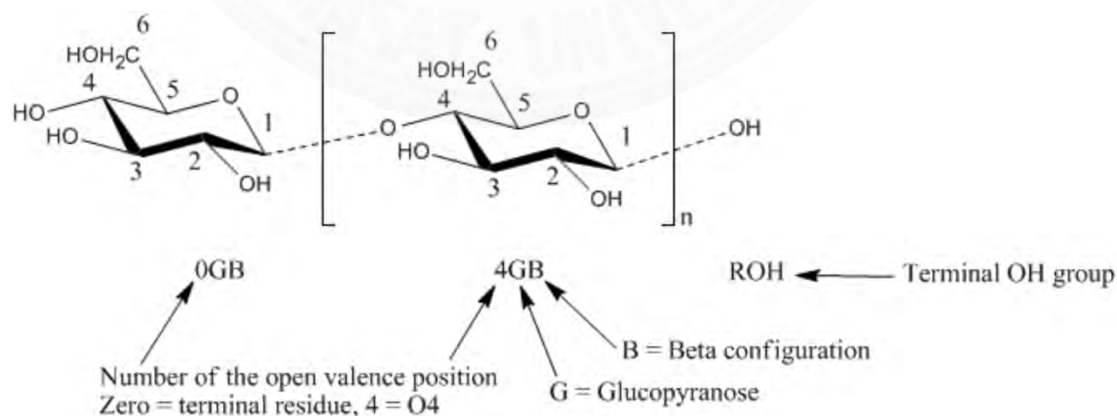


Figure D.2 Illustration of the GLYCAM naming convention applied to cellobiose

BIOGRAPHY

Name	Ms. Ornin Srihakulung
Date of Birth	July 25, 1985
Education	2006: Bachelor of Engineering (Industrial Engineering) Chiangmai University 2014: Master of Engineering (Metallurgy Engineering) Chulalongkorn University 2018: Doctor of Philosophy Information Science Japan Advanced Institute of Technology

Publications

- Ornin, S., Maezono, R., Pisanu, T., Waree, K., Apichart, I., and Luckhana, L. (2018). Host-Guest Interactions of Plumbagin with β -cyclodextrin, Dimethyl- β -cyclodextrin and Hydroxypropyl- β -cyclodextrin: Semi-Empirical Quantum Mechanical PM6 and PM7 Methods, Sci. Pharm. 86(2), 20; https://doi.org/10.3390/sci_pharm86020020
- Ornin, S., Luckhana, L., Pisanu, T., Waree, K., Apichart, I., and Maezono, R. (2017). Theoretical investigation of molecular calculations on inclusion complexes of plumbagin with β -cyclodextrin, in 2017 Fourth Asian Conference on Defence Technology - Japan (ACDTJ), pp. 1-5. doi: 10.1109/ACDTJ.2017.8259589